

Chiral kinematic theory and converse vortical effects

Kai Chen, Swadeepan Nanda, and Pavan Hosur

Department of Physics and Texas Center for Superconductivity, University of Houston, Houston, TX 77204

(Dated: November 14, 2024)

Response theories in condensed matter typically describe the response of an electron fluid to external electromagnetic fields, while perturbations on neutral particles are often designed to mimic such fields. Here, we study the response of fermions to a space-time-dependent velocity field, thereby sidestepping the issue of gauge charge. First, we use a semiclassical chiral kinematic theory to obtain the local density of current and extract the orbital magnetization. The theory immediately predicts a "converse vortical effect," defined as an orbital magnetization driven by linear velocity. It receives contributions from magnetic moments on the Fermi surface and the Berry curvature of the occupied bands. Then, transcending semiclassics via a complementary Kubo formalism reveals that the uniform limit of a clean system receives only the Berry curvature contribution while other limits sense the Fermi surface magnetic moments too. We propose CoSi as a candidate material and suggest magnetometry of a sample under a thermal gradient to detect the effect. Overall, our study sheds light on the effects of a space-time-dependent velocity field on electron fluids and paves the way for exploring quantum materials using new probes and perturbations.

I. Introduction

Response theories, a fundamental framework in physics, explore how physical systems dynamically respond to external perturbations. In the context of quantum materials, they describe a myriad of properties ranging from conventional ones such as longitudinal conductivity and magnetization, to topological ones such as the quantized Hall conductivity of two-dimensional (2D) insulators and the half-quantum Hall effect on the surface of 3D topological insulators^{1,2}. As most responses involve the constituent electrons responding to external electromagnetic fields, response theories provide a bridge from microscopic quantum phenomena to macroscopic material properties and facilitate the design of novel functional materials tunable by these fields.

A striking family of responses with deep topological roots are the so-called chiral responses. Chirality refers to an intrinsic handedness of the system and is non-zero only in systems that break all improper symmetries including parity, such as an isolated Weyl fermion. Thus, chiral responses were initially explored in various contexts in fundamental physics ranging from left-handed neutrinos^{3,4} and parity violation^{5,6} in the Standard Model to the fluid dynamics of rotating blackholes⁷⁻¹⁰ and axion models of dark matter¹¹⁻¹³. Since the discovery of Weyl semimetals (WSMs), whose band structure contains intersections around which the excitations resemble relativistic Weyl fermions,¹⁴⁻²¹ interest has mushroomed in chiral responses in condensed matter²²⁻²⁷. Most chiral responses can be traced to topological chiral anomalies, defined as the breakdown of classical conservation laws upon quantization of chiral fermion²⁷⁻³³. The anomalies, too, were first explored in high-energy physics, but have found remarkable applications in topological condensed matter, particularly in Weyl and Dirac semimetals, manifesting as exotic transport phenomena³⁴⁻³⁹.

An important and fundamental chiral response is the chiral vortical effect (CVE), defined as an axial current driven by rotation in a chiral fluid^{40,41}. Since the advent of WSMs, it has been derived for general chiral band

structures⁴²⁻⁴⁴, has been extended to arbitrary spacetime-dependent rotation, and motivated a related effect dubbed the gyrotropic vortical effect (GVE)⁴⁵. Moreover, the generalizations have revealed the origins of the effect in the Berry curvature $\mathbf{\Omega}_n(\mathbf{k})$ and orbital magnetic moment $\mathbf{m}_n^{\text{orb}}(\mathbf{k})$ of the relevant bands.

A powerful framework that captures chiral responses including the topological nature of the chiral anomaly is the semiclassical chiral kinetic theory^{40,46-54}. Moreover, using analogies between electromagnetic and fictitious non-inertial fields, such as the similarity between the classical Lorentz and Coriolis forces, chiral kinetic theory can also encompass certain responses of Weyl fermions to space and time-dependent velocity fields $\mathbf{v}(\mathbf{r}, t)$ including the CVE^{40,44,45,55-57}. Such kinematic responses – chiral and otherwise – are routinely used to simulate gauge fields for neutral ultracold atoms⁵⁸⁻⁶¹. They are arguably more fundamental than electromagnetic responses as they do not rely on a well-defined conserved charge and exist, for instance, even for superconducting quasiparticles whose charge is ill-defined. However, while the analogies are established for non-relativistic and relativistic free particles in vacuum, they are unknown for electrons in general band structures. Thus, a general description of kinematic responses independently of electromagnetic analogies is highly desirable.

In this paper, we study the linear response of electrons in general band structures to a space-time dependent velocity field, $\mathbf{v}(\mathbf{r}, t)$. Interestingly, if the band structure is chiral, we show that the velocity field gives rise to an orbital magnetization. The effect is the opposite of the vortical effect in a sense that we specify, and we dub the phenomenon the converse vortical effect.

We begin by introducing the converse vortical effect via an analogy with the vortical effect in Sec. II. We then use a semiclassical chiral kinematic theory to derive this effect in Sec. III. In particular, we calculate the orbital magnetization $\mathbf{M}^{\text{orb}} = \chi^{\text{orb}} \cdot \mathbf{v}$, where χ^{orb} denotes the susceptibility of orbital magnetization to the velocity field. Then, in Sec. IV, we employ a complementary, quantum mechanical Kubo approach to compute the linear

response function at general frequencies ω and momenta \mathbf{q} of the velocity field in the presence of a phenomenological quasiparticle lifetime τ . This approach shows that the uniform limit of a clean system, defined by $q = 0$, $\omega \rightarrow 0$ and $|\omega\tau| \gg 1$, has a response purely governed by $\Omega_n(\mathbf{k})$ of the occupied bands. In contrast, other orders of limits of $\omega \rightarrow 0$, $q \rightarrow 0$ and $\tau \rightarrow \infty$ also acquire contributions from $\mathbf{m}_n^{\text{orb}}(\mathbf{k})$ on the Fermi surface. We refer to the response in the uniform limit ($q \rightarrow 0$ before $\omega \rightarrow 0$) as the converse gyrotropic vortical effect (cGVE), and that in the static limit ($q \rightarrow 0$ after $\omega \rightarrow 0$) as the converse chiral vortical effect (cCVE). In Sec. V, we calculate the cGVE and cCVE in Weyl fermions, and close by proposing CoSi as a candidate material to observe both the cGVE and cCVE in Sec. VI.

II. Vortical and Converse Vortical Effects

The vortical and converse vortical effects can be heuristically likened to a bolt and nut analogy. When the head of a bolt is rotated faster, it generates more torque, which transforms into linear force, enabling the bolt to move faster inside the nut. This phenomenon of linear motion driven by circular resembles the vortical effect. Conversely, when a bolt has a higher linear speed inside the nut, its head gains faster circular rotation. This is the classical counterpart of the converse vortical effect. The converse vortical effect is a quantum phenomenon and, as we will see later, relies on the Berry curvature and magnetic moment of Bloch electrons.

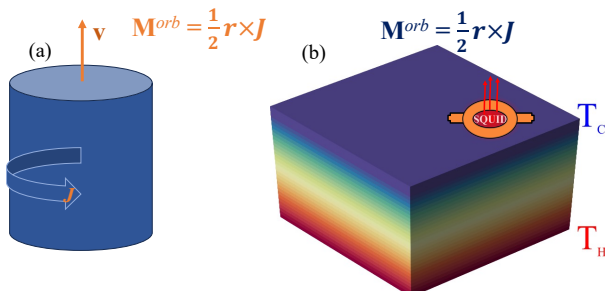


Figure 1. Color online. (a) Schematic depiction of the converse vortical effect. (b) Device geometry for observing the converse vortical effect: The temperature difference propels electrons, inducing their motion with velocity \mathbf{v} . The resulting magnetization can be observed aligned with the velocity field.

To better understand the converse effects – and their nomenclature – in a broader context, let us recap other closely related effects. First, continuum Weyl fermions in a \mathbf{B} -field exhibit the chiral magnetic effect (CME), arising from the chiral anomaly and manifesting as a current parallel to \mathbf{B} ^{14,15,23}, unlike conventional charged particles that undergo circular motion in an orthogonal plane. In WSMs, the CME vanishes at equilibrium due to Bloch’s theorem^{62,63} that forbids equilibrium current densities but persists in non-equilibrium steady states with unequal Fermi levels for left- and right-handed Weyl nodes.

Reconciling the continuum and lattice manifestations of the CME involved considering non-zero \mathbf{q} and ω responses. The original CME emerges in the static limit and relies on the existence of Weyl nodes while the uniform limit revealed a new effect, termed the gyrotropic magnetic effect (GME)^{24,64}, that corresponds to a current along a time-dependent \mathbf{B} -field and exists for general band structures. Analogous to the CME, the CVE corresponds to the static limit and represents another anomaly-induced transport phenomenon^{41,44,57,65–69}, namely, the dissipationless axial current proportional to $\mathcal{V} = \frac{1}{2} \nabla \times \mathbf{v}$. Similarly, the gyrotropic vortical effect (GVE) was recently defined as the extension of the CVE to the uniform limit that crucially relies on the time-dependence of \mathcal{V} ⁴⁵. Both vortical effects exist at equilibrium for general band structures regardless of Weyl nodes. In short, the CME and GME are defined by $\mathbf{J} \propto \mathbf{B}$ in different limits whereas the CVE and GVE are given by $\mathbf{J} \propto \mathcal{V}$ in these limits.

The GME inspires an effect dubbed the inverse GME, defined as magnetization proportional to the vector potential, $\mathbf{M} \propto \mathbf{A}$ with a response function that is the matrix inverse of that of the GME⁶⁴. The CME lacks an inverse response since a static \mathbf{A} is a pure gauge field. The GME and its inverse are related by an interchange of conjugate variables, $\mathbf{J} \leftrightarrow \mathbf{A}$ and $\mathbf{B} \leftrightarrow \mathbf{M}$, followed by an interchange of the left- and right-hand sides. Physically, this means the field \mathbf{A} conjugate to the GME response \mathbf{J} drives the inverse GME, and vice versa. This pattern suggests analogous inverse kinematic responses where a linear momentum \mathbf{K} , conjugate to the linear current \mathbf{J} , drives an angular momentum \mathbf{L} that is conjugate to the angular velocity \mathcal{V} . While such responses presumably exist, our focus is on a distinct class of effects: unlike the inverse effects, the converse effects correspond to an interchange of responding and driving fields without conjugation. Thus, we wish to compute an angular velocity \mathcal{V} driven by a linear velocity \mathbf{v} . However, we compute a slightly different quantity that also characterizes rotational motion, namely, $\mathbf{M}^{\text{orb}} \equiv \frac{1}{2} \mathbf{r} \times \mathbf{J}$ as a proxy for \mathcal{V} , as \mathbf{M}^{orb} is directly measurable in experiments and easier to compute than \mathcal{V} . Note that in general, \mathbf{L} , not \mathbf{M}^{orb} , is conjugate to \mathcal{V} and the diamagnetic contribution to the current is $\nabla \times \mathbf{M}^{\text{orb}}$. Only in simple cases such as a classical current loop, $\mathbf{L} \propto \mathbf{M}^{\text{orb}}$, and \mathbf{M}^{orb} and \mathbf{L} are used interchangeably upto overall constants.

III. Chiral kinematic theory

In this section, we first employ the semiclassical wavepacket dynamics method⁷⁰ to obtain the response function for the converse vortical effect. We will first derive the equations of motion (EM) for electrons subjected to a space-time dependent velocity field. Next, we utilize these equations to compute the local density of current (LDC) following the general method proposed in Ref.⁷¹. The local density of a physical observable provides a convenient way to compute that observable. Given that orbital magnetization can induce current, the LDC can provide insights into the distribution of orbital magnetization, which is the primary focus of this work.

Let us consider electrons in periodic crystals governed

by the Hamiltonian $H_0(\hat{\mathbf{k}}, \mathbf{r})$, influenced by a space-time dependent velocity field $\mathbf{v}(\mathbf{r}, t)$ that is significantly smaller than typical band velocities. Here, $\hat{\mathbf{k}} \equiv -i\nabla_{\mathbf{r}}$ is the continuum momentum operator and has eigenvalue \mathbf{k} . As shown in Appendix A, the effect of the velocity field can be captured by a perturbed Hamiltonian $H_0(\hat{\mathbf{k}}, \mathbf{r}) - \hat{\mathbf{k}} \cdot \mathbf{v}(\mathbf{r}, t)$ that describes dynamics in a frame moving with the fluid. Physically, this form is simply a consequence of $\hat{\mathbf{k}}$ being the generator of continuum translations and can be intuited as a Galilean boost.

To derive the LDC, we introduce an auxiliary background momentum field $\mathbf{K}(\mathbf{r}, t)$, which shifts $\mathbf{k} \rightarrow \mathbf{k} - \mathbf{K}$ and is conjugate to the number current operator $\hat{\mathbf{J}} \equiv \nabla_{\hat{\mathbf{k}}} H_0$. In $U(1)$ gauge theories, \mathbf{K} simply corresponds to the gauge field multiplied by the gauge charge. However, a background momentum is more general concept, essentially defining a spacetime-dependent reference point in momentum space about which the dynamics occurs, and is well-defined for neutral particles too.

Mimicking gauge theories, this introduces an additional perturbation $-\hat{\mathbf{J}} \cdot \mathbf{K}(\mathbf{r}, t)$ into the Hamiltonian. We emphasize that the auxiliary momentum field \mathbf{K} is introduced solely to calculate the LDC and determine the orbital magnetization. As is standard for response theory calculations, it will be taken to zero once the response functions are formally setup through appropriate functional derivatives. The total Hamiltonian is now

$$\hat{H}_{\text{tot}} = H_0(\hat{\mathbf{k}}, \mathbf{r}) - \hat{\mathbf{k}} \cdot \mathbf{v}(\mathbf{r}, t) - \hat{\mathbf{J}} \cdot \mathbf{K}(\mathbf{r}, t). \quad (1)$$

Using the standard semiclassical wave-packet method (see Ref.⁷⁰ and Appendix B for details), and assuming that both \mathbf{v} and \mathbf{K} vary slowly in space and time, the action for the wave packet takes the form $S = \int L dt$, with the Lagrangian L given by

$$L = \mathcal{A}_t + \dot{\mathbf{r}}_c \cdot \mathcal{A}_{\mathbf{r}_c} + \dot{\mathbf{k}}_c \cdot \mathcal{A}_{\mathbf{k}_c} + \dot{\mathbf{k}}_c \cdot \mathbf{r}_c - E. \quad (2)$$

where \mathbf{r}_c and \mathbf{k}_c are the position and momentum of the center of mass of the wave packet. Additionally, $\mathcal{A}_\alpha = \langle u_n | i\partial_\alpha | u_n \rangle$ for $\alpha \in \{\mathbf{k}_c, \mathbf{r}_c, t\}$ represents the Berry connections, and the energy E is

$$E = \epsilon_n + \text{Im} \langle \partial_{k_i} u_n | \epsilon_n - \hat{H} | \partial_{\mathbf{v}} u_n \rangle \cdot \partial_{r_i} \mathbf{v} + \text{Im} \langle \partial_{k_i} u_n | \epsilon_n - \hat{H} | \partial_{\mathbf{K}} u_n \rangle \cdot \partial_{r_i} \mathbf{K}. \quad (3)$$

where the Hamiltonian $\hat{H} = H_0(\hat{\mathbf{k}}, \mathbf{r}) - \hat{\mathbf{k}} \cdot \mathbf{v}(\mathbf{r}_c, t) - \hat{\mathbf{J}} \cdot \mathbf{K}(\mathbf{r}_c, t)$ is obtained by evaluating the \mathbf{v} and \mathbf{K} in \hat{H}_{tot} at the center of mass position \mathbf{r}_c of the wave packet, and ϵ_n and $|u_n\rangle$ represent the n th eigenvalue and eigenstate of \hat{H} , respectively. Summation over the repeated index i is implied henceforth and to simplify the notation, we will omit the band index n and the index c in \mathbf{r}_c . Since the wave packet size is much larger than the unit cell, we effectively enter the continuum limit. Consequently, we will replace \mathbf{k}_c with \mathbf{k} in the following discussion.

To obtain the EM, we apply the Euler-Lagrange equations to the Lagrangian L . The EM are given by:

$$\begin{cases} \dot{\mathbf{r}} = \partial_{\mathbf{k}} E - \Omega_{\mathbf{k}t} - \Omega_{\mathbf{k}\mathbf{r}} \cdot \dot{\mathbf{r}} - \Omega_{\mathbf{k}\mathbf{k}} \cdot \dot{\mathbf{k}}, \\ \dot{\mathbf{k}} = -\partial_{\mathbf{r}} E + \Omega_{\mathbf{r}t} + \Omega_{\mathbf{r}\mathbf{r}} \cdot \dot{\mathbf{r}} + \Omega_{\mathbf{r}\mathbf{k}} \cdot \dot{\mathbf{k}}. \end{cases} \quad (4)$$

Here, $\Omega_{\alpha\beta}^{ij} = \partial_{\alpha_i} \mathcal{A}_\beta^j - \partial_{\beta_j} \mathcal{A}_\alpha^i$ represents the Berry curvature in the generalized space spanned by $\mathbf{r}, \mathbf{k}, t$.

The LDC, see Eq. (10) in the supplementary material of Ref.⁷¹, can be expressed as:

$$\begin{aligned} \rho_{\text{loc}}^{\mathbf{J}} &= \lim_{\mathbf{K} \rightarrow 0} \left\{ - \int d\mathbf{k} Df \left[\frac{\partial E}{\partial \mathbf{K}} - \Omega_{\mathbf{K}\mathcal{T}} \right] \right. \\ &\quad \left. - \nabla_{\mathbf{r}} \cdot \int d\mathbf{k} Df \text{Im} \langle \partial_{\mathbf{k}} u | \epsilon - \hat{H} | \partial_{\mathbf{K}} u \rangle \right\}, \end{aligned} \quad (5)$$

where $\int d\mathbf{k} \equiv \int \frac{d\mathbf{k}}{(2\pi)^d}$, with d being the spatial dimension of the system, and $\Omega_{\mathbf{K}\mathcal{T}} = \dot{\mathbf{k}} \cdot \Omega_{\mathbf{K}\mathbf{k}} + \dot{\mathbf{r}} \cdot \Omega_{\mathbf{K}\mathbf{r}} + \Omega_{\mathbf{K}t}$, $D \equiv 1 + \Omega_{k_i r_i}$ is a modified phase space measure and the local equilibrium distribution is given by $f = \frac{1}{1 + e^{\beta(\epsilon - \mathbf{k} \cdot \mathbf{v})}}$, where $\beta = T^{-1}$ is the inverse temperature. By performing integration by parts and using the EM, at constant temperature and chemical potential, the LDC reduces to (see Appendix B for details)

$$\begin{aligned} \rho_{\text{loc}}^{\mathbf{J}} &= -\nabla_{\mathbf{r}} \cdot \int d\mathbf{k} (-g\Omega_{\mathbf{k}\mathbf{k}} + f \text{Im} \langle \partial_{\mathbf{k}} u | \epsilon - \hat{H} | \partial_{\mathbf{k}} u \rangle) \\ &\quad + \int d\mathbf{k} f \Omega_{\mathbf{k}t} \equiv -\partial_i M^{i\mathbf{J}} + \int d\mathbf{k} f \Omega_{\mathbf{k}t}, \end{aligned} \quad (6)$$

Observe that for a time-dependent external field, the LDC includes contributions from the Berry curvature $\Omega_{\mathbf{k}t}$. This term accounts for the charge pumping current⁷². For a filled band, using a gauge where \mathcal{A}_t is periodic in the Brillouin zone, the last term in $\rho_{\text{loc}}^{\mathbf{J}}$ is formulated as:

$$\int d\mathbf{k} \Omega_{\mathbf{k}t} = -\partial_t \int d\mathbf{k} \mathcal{A}_{\mathbf{k}} = -\partial_t \mathbf{P}, \quad (7)$$

where \mathbf{P} is the polarization. Thus, this term corresponds to the current induced by polarization. The quantity

$$M^{i\mathbf{J}j} = \int d\mathbf{k} (-g\Omega_{k_i k_j} + f \text{Im} \langle \partial_{k_i} u | \epsilon - \hat{H} | \partial_{k_j} u \rangle) \equiv M_{ij}, \quad (8)$$

represents the dipole density tensor of current or the orbital magnetization tensor⁷¹. Its vector form is

$$M_l^{\text{orb}} = \frac{\epsilon_{lij} M_{ij}}{2} = \int d\mathbf{k} (f m_l^{\text{orb}} - g \Omega_l(\mathbf{k})), \quad (9)$$

where $\Omega_l(\mathbf{k})$ is the l -th component of the Berry curvature, and m_l^{orb} is the l -th component of the orbital magnetic moment. The function g is given by:

$$g = -\frac{1}{\beta} \ln[1 + e^{-\beta(\epsilon - \mathbf{k} \cdot \mathbf{v})}]. \quad (10)$$

Finally, by reintroducing the band index and summing the contributions of each band, we obtain the density of

orbital magnetization

$$\mathbf{M}^{\text{orb}} = \sum_n \int d\mathbf{k} \left\{ f \mathbf{m}_n^{\text{orb}} + \frac{1}{\beta} \ln[1 + e^{-\beta(\epsilon_{n,\mathbf{k}} - \mathbf{k} \cdot \mathbf{v})}] \Omega_n \right\}. \quad (11)$$

For a parabolic band with Berry phases due to internal degrees of freedom, the same equation for orbital magnetization can be obtained using the free energy density (see Appendix C for details). The converse vortical effect refers to the response of orbital magnetization to \mathbf{v} in linear order. Formally Taylor expanding in \mathbf{v} leads to:

$$\begin{aligned} \mathbf{M}^{\text{orb}}(\mathbf{v}) &= \sum_n \int_{\mathbf{k}} \mathbf{m}_n^{\text{orb}} f \\ &\quad + \frac{1}{\beta} \int_{\mathbf{k}} \Omega_n \ln \left(1 + e^{-\beta(\epsilon_{n,\mathbf{k}} - \mathbf{k} \cdot \mathbf{v})} \right) \\ &\equiv \mathbf{M}_0^{\text{orb}} + \chi^{\text{orb}} \cdot \mathbf{v} + O(\mathbf{v}^2), \end{aligned} \quad (12)$$

where the \mathbf{v} -independent term $\mathbf{M}_0^{\text{orb}}$ denotes the intrinsic equilibrium magnetization and the tensor χ^{orb} is the desired response function for the converse vortical effect. At $T = 0$, $f = \Theta(-\epsilon_{n,\mathbf{k}} + \mathbf{k} \cdot \mathbf{v})$, and χ^{orb} reduces to:

$$\begin{aligned} \chi_{ij}^{\text{orb}} &= \sum_n \int_{\mathbf{k}} m_{n,i}^{\text{orb}} \delta(\epsilon_{n,\mathbf{k}}) k_j \\ &\quad + \sum_n \int_{\mathbf{k}} \Theta(-\epsilon_{n,\mathbf{k}}) \Omega_{n,i} k_j \equiv \chi_{ij}^{\text{Fs}} + \chi_{ij}^{\text{occ}}. \end{aligned} \quad (13)$$

The equation above reveals that the magnetic susceptibility is determined by the orbital magnetic moment of electrons on the Fermi surface (indicated as χ_{ij}^{Fs}) as well as the Berry curvature of the occupied bands (indicated as χ_{ij}^{occ}). Interestingly, this response function takes the same form as the vortical effect⁴⁵. However, they represent distinct responses. The vortical effect is defined as the axial current response to angular velocity while the converse vortical effect is the orbital magnetization response to linear velocity.

IV. Kubo Formula for Converse Vortical Effect

The Kubo formula provides a fundamental theoretical framework for analyzing the linear response of a system to external perturbations. In this section, we apply the Kubo formula to compute χ_{ij}^{orb} for a space-time-dependent velocity field, considering general values of \mathbf{q} and ω , and incorporating the effects of quasiparticle lifetime τ . The motivation for using the Kubo formula lies in its ability to elucidate the system's response across different limits (e.g., static, uniform), providing valuable insights into the fundamental physical mechanisms governing the orbital magnetization.

The Bloch energy and wave function for the n -th band are given by $\epsilon_{n,\mathbf{k}}$ and $\psi_{n,\mathbf{k}}(\mathbf{r}) = \psi_{n,\mathbf{k}}(\mathbf{R} + \boldsymbol{\rho}) = N^{-1/2} e^{i\mathbf{k} \cdot (\mathbf{R} + \boldsymbol{\rho})} u_{n,\mathbf{k}}(\boldsymbol{\rho})$, respectively, where \mathbf{k} represents the Bloch momentum of electrons, and \mathbf{R} denotes the coordinates of the unit cells, $\boldsymbol{\rho}$ represents position within each unit cell and N is the total number of unit cells. In

this basis, the matrix elements of the velocity-induced perturbation $H_1 = -\hat{\mathbf{k}} \cdot \mathbf{v}(\mathbf{r}, t)$ with $\hat{\mathbf{k}}$ denoting the momentum operator, are $\langle \psi_{n,\mathbf{k}} | H_1 | \psi_{m,\mathbf{k}+\mathbf{q}} \rangle = (2\pi)^3 \langle u_{n,\mathbf{k}} | (\mathbf{k} - i\nabla_{\boldsymbol{\rho}}) | u_{m,\mathbf{k}+\mathbf{q}} \rangle \cdot \mathbf{v}(\mathbf{q}, t)$, where $\mathbf{v}(\mathbf{q}, t)$ is $\mathbf{v}(\mathbf{r}, t)$ Fourier transformed to momentum space. Thus, it is convenient to introduce the operator $\hat{\mathbf{Q}} = \mathbf{k} - i\nabla_{\boldsymbol{\rho}}$ and write $H_1 = -\hat{\mathbf{Q}} \cdot \mathbf{v}$. Unlike the continuum perturbation $-\mathbf{k} \cdot \mathbf{v}$, H_1 respects the Brillouin Zone periodicity and can be viewed as the kinematic analog of minimal coupling $\mathbf{J} \cdot \mathbf{A}$ that is well-defined on a lattice through Peierl's substitution⁴⁵.

To calculate χ_{ij}^{orb} , we Fourier transform $\mathbf{M}^{\text{orb}} = \frac{1}{2} \mathbf{r} \times \mathbf{J}$ to Bloch momentum and Matsubara frequencies, $\mathbf{M}^{\text{orb}}(\mathbf{q}, iq_n) = \frac{i}{2} \nabla_{\mathbf{q}} \times \mathbf{J}(\mathbf{q}, iq_n)$, and compute the susceptibility, $\chi_{ij}^{\text{orb}}(\mathbf{q}, iq_n) = \frac{\partial M_i^{\text{orb}}}{\partial v_j}(\mathbf{q}, iq_n)$ with i and j denoting spatial components. The basic one-loop diagram yields

$$\begin{aligned} \chi_{ij}^{\text{orb}}(\mathbf{q}, iq_n) &= -\epsilon_{i\mu\nu} i \partial_{q_\mu} \frac{1}{2\beta} \sum_{\nu_n} \int_{\mathbf{k}} \\ &\quad \text{tr} [J_\nu(\mathbf{k} + \mathbf{q}) G_0(\mathbf{k}, i\nu_n) G_0(\mathbf{k} + \mathbf{q}, i\nu_n + iq_n) Q_j] \end{aligned} \quad (14)$$

where $G_0(\mathbf{k}, i\nu_n) = [i\nu_n - H_0(\mathbf{k}) + i\text{sgn}(\nu_n)/2\tau]^{-1}$ is the unperturbed Matsubara Green's function, the elements of the matrix Q_j are $Q_j^{mn} = \langle u_{m,\mathbf{k}} | \hat{Q}_j | u_{n,\mathbf{k}+\mathbf{q}} \rangle$, $J_\nu(\mathbf{k}) = \frac{\partial H_0(\mathbf{k})}{\partial k_\nu}$ is the current operator and repeated indices are summed. The retarded response function follows from analytically continuing $iq_n \rightarrow \omega + i0^+$. The Matsubara sum yields

$$\begin{aligned} \chi_{ij}^{\text{orb}}(\mathbf{q}, iq_n) &= -\frac{1}{2} \epsilon_{i\mu\nu} i \partial_{q_\mu} \int_{\mathbf{k}} \sum_{n,m} S_{m,n}(\mathbf{k}, \mathbf{q}, iq_n) \\ &\quad \langle u_{n,\mathbf{k}+\mathbf{q}} | J_\nu(\mathbf{k} + \mathbf{q}) | u_{m,\mathbf{k}} \rangle Q_j^{mn}, \end{aligned} \quad (15)$$

where

$$\begin{aligned} S_{m,n}(\mathbf{k}, \mathbf{q}, iq_n) &= \frac{1}{\beta} \sum_{\nu_n} \frac{1}{i\nu_n - \epsilon_{m,\mathbf{k}} + i \frac{\text{sgn}(\nu_n)}{2\tau}} \\ &\quad \frac{1}{i\nu_n + iq_n - \epsilon_{n,\mathbf{k}+\mathbf{q}} + i \frac{\text{sgn}(\nu_n + q_n)}{2\tau}}. \end{aligned} \quad (16)$$

At zero temperature, the off-diagonal elements of the matrix Q_j couple to the inter-band orbital magnetization matrix of the Bloch electrons⁷³, contributing to the orbital magnetization (for more details, see the Appendix D).

We now focus on the zero-temperature regime in the context of both the nearly-free electron approximation and the deep tight-binding approximation⁴⁵. In the deep tight-binding approximation, within the unit cell, the lattice potential can be approximated by the form $V(\boldsymbol{\rho}) = \sum_j V_j \delta(\boldsymbol{\rho} - \boldsymbol{\rho}_j)$, where $\boldsymbol{\rho}_j$ and $\boldsymbol{\rho}$ denote discrete points and the continuous position variable within a unit cell, respectively. The Bloch function $u_{n,\mathbf{k}}(\boldsymbol{\rho}) = \sum_j u_{n,\mathbf{k}} \phi_j(\boldsymbol{\rho})$, where \mathbf{k} is within the first Brillouin zone, and the function $\phi_j(\boldsymbol{\rho}) \approx e^{-\sqrt{2|E|}|\boldsymbol{\rho} - \boldsymbol{\rho}_j|}$, with E and m denoting the energy and mass of the electron, respectively. The term $\langle \phi_i | i\nabla_{\boldsymbol{\rho}} | \phi_j \rangle \ll 1$ if $i \neq j$ and $\langle \phi_j | i\nabla_{\boldsymbol{\rho}} | \phi_j \rangle = 0$

Limit	Definition	χ_{ij}^{occ}	χ_{ij}^{Fs}	$\chi_{ij}^{\text{Weyl}} = \chi_{ij}^{\text{occ}} + \chi_{ij}^{\text{Fs}}$
Uniform, clean	$\tilde{v}q \ll \omega , 1 \ll \omega \tau$, arbitrary $\tilde{v}q\tau$	$\sum_n \int_k \Omega_{n,i}(\mathbf{k})\Theta(-\epsilon_{n,\mathbf{k}})k_j$	0	$\frac{1}{6}\chi_{ij}^{\mathcal{C}} = \frac{1}{6}\chi_{ij}^{\mathcal{C}} + 0$
Static, clean	$ \omega \ll \tilde{v}q, 1 \ll \tau\tilde{v}q$, arbitrary $\omega\tau$	$\sum_n \int_k \Omega_{n,i}(\mathbf{k})\Theta(-\epsilon_{n,\mathbf{k}})k_j$	$\sum_n \int_k m_{n,i}^{\text{orb}}(\mathbf{k})\delta(\epsilon_{n,\mathbf{k}})k_j$	$\frac{1}{2}\chi_{ij}^{\mathcal{C}} = \frac{1}{3}\chi_{ij}^{\mathcal{C}} + \frac{1}{6}\chi_{ij}^{\mathcal{C}}$
Uniform, disorder	$\tilde{v}q\tau \ll \omega \tau \ll 1$	$\sum_n \int_k \Omega_{n,i}(\mathbf{k})\Theta(-\epsilon_{n,\mathbf{k}})k_j$	$\sum_n \int_k m_{n,i}^{\text{orb}}(\mathbf{k})\delta(\epsilon_{n,\mathbf{k}})k_j$	$\frac{1}{2}\chi_{ij}^{\mathcal{C}} = \frac{1}{3}\chi_{ij}^{\mathcal{C}} + \frac{1}{6}\chi_{ij}^{\mathcal{C}}$
Static, disorder	$ \omega \tau \ll \tilde{v}q\tau \ll 1$	$\sum_n \int_k \Omega_{n,i}(\mathbf{k})\Theta(-\epsilon_{n,\mathbf{k}})k_j$	$\sum_n \int_k m_{n,i}^{\text{orb}}(\mathbf{k})\delta(\epsilon_{n,\mathbf{k}})k_j$	$\frac{1}{2}\chi_{ij}^{\mathcal{C}} = \frac{1}{3}\chi_{ij}^{\mathcal{C}} + \frac{1}{6}\chi_{ij}^{\mathcal{C}}$

Table I. Summary of results as $q \rightarrow 0$ and $\omega \rightarrow 0$ at various orders is presented for general band structures. In the definition column, $\tilde{v} \equiv |\nabla_{\mathbf{k}}\epsilon_{n,\mathbf{k}}|$. The last column represents the orbital magnetization for an isotropic Weyl fermion with a velocity of $\tilde{v} = v_F$, chiral charge \mathcal{C} , and chemical potential μ relative to the Weyl node. Here, $\chi_{ij}^{\mathcal{C}} = \mathcal{C} \left(\frac{\mu}{2\pi v_F}\right)^2 \delta_{ij}$.

since $\phi_j(\boldsymbol{\rho})$ have definite parity, hence, the inner product $\langle u_{n,\mathbf{k}} | i\nabla_{\boldsymbol{\rho}} | u_{n,\mathbf{k}'} \rangle$ is exponentially small. Under these conditions, the Fermi distribution function $f(\epsilon_{n,\mathbf{k}})$ and Q_j^{mn} simplify to $\Theta(-\epsilon_{n,\mathbf{k}})$ and $k_j\delta_{mn}$, respectively. The difference between various orders of limits of $\omega \rightarrow 0$, $q \rightarrow 0$ and $\tau \rightarrow \infty$ is determined by the behavior of $S_{m,n}$ in these limits. In the static limit ($\omega \rightarrow 0$ followed by $q \rightarrow 0$), we find χ_{ij}^{orb} reduces to Eq. (13) derived using semiclassical chiral kinematic theory for both $v_F q \tau \gg 1$ and $v_F q \tau \ll 1$, where v_F is a typical band velocity. In contrast, the dirty uniform limit, ($\mathbf{q} \rightarrow 0$ followed by $\omega \rightarrow 0$ with $|\omega\tau| \ll 1$), leads to Eq. (13) while the clean uniform limit ($\mathbf{q} \rightarrow 0$ followed by $\omega \rightarrow 0$ with $|\omega\tau| \gg 1$) gives:

$$\chi_{ij}^{\text{orb}} = \int \sum_n \Theta(-\epsilon_{n,\mathbf{k}}) \Omega_{n,i}(\mathbf{k}) k_j \quad (17)$$

Thus, χ_{ij}^{orb} in this limit is solely determined by $\Omega_n(\mathbf{k})$ of occupied bands. It is worth noting that the $\Omega_n(\mathbf{k})$ contribution vanishes for a filled band in the continuum limit at zero temperature, where $\hat{Q}_j \rightarrow \hat{k}_j$ and $u_{n,\mathbf{k}}$ become \mathbf{k} -independent as $k \rightarrow \infty$, similarly to the GVE⁴⁵. Therefore, only partially filled bands contribute to \mathbf{M}^{orb} in any limit. The results are summarized in Table I. However, in a disordered electron fluid with relatively short τ , both the Berry curvature of the occupied bands and the orbital moment of electrons on the Fermi surface contribute to the magnetic susceptibility in both the static and uniform limits. This magnetic susceptibility takes the same form as described in Eq. (13), acquiring the combined effects of the Berry curvature and the orbital moment. In analogy with the CVE and the GVE, we refer to the two results for the converse effects, Eqs. (13) and (17) as the cCVE and the cGVE, respectively.

V. cCVE and cGVE of Weyl fermions

We now evaluate χ_{ij}^{orb} for a single, isotropic, continuum Weyl fermion with chirality $\mathcal{C} = \pm 1$. The effective Hamiltonian is given by $H(\mathbf{k}) = \mathcal{C}\mathbf{k} \cdot \boldsymbol{\sigma} - \mu - \mathbf{k} \cdot \mathbf{v}$, where $\boldsymbol{\sigma}$ represents the Pauli matrices and μ is the chemical potential relative to the Weyl node and \mathbf{v} . The results at $T = 0$ are stated in Table I. Since the effect is proportional to the chirality \mathcal{C} and μ^2 , which are odd and even under improper symmetries, respectively, all improper symmetries must be broken for a material with pairs of

Weyl fermions, rendering the material chiral overall in addition to each Weyl node being chiral.

VI. Experimental realization

To experimentally observe the converse vortical effects, we propose a simple experiment sketched in Fig. 1. This is significantly simpler than the curved geometries required for the vortical effects⁴⁵. By leveraging a temperature difference gradient ($\nabla T \approx 1\text{K}/\mu\text{m}$) and a Seebeck coefficient ($S = 100\text{a}\mu\text{V}/\text{K}$), we generate an electric field strength of $|\mathbf{E}| = 0.1\text{V}/\text{m}$, driving the motion of electrons relative to the lattice. Consequently, \mathbf{M}^{orb} aligns with $\mathbf{v} = \mu_{\text{mob}}\mathbf{E}$, with μ_{mob} representing the mobility of the system. For a WSM with typical parameter values such as $\mu_{\text{mob}} = 10^5\text{cm}^2/(\text{Vs})$, $v_F = 10^5\text{m}/\text{s}$, and Fermi energy differences $\mu_{\pm} = (0.5 \pm 0.025)\text{eV}$ relative to the left-handed/right-handed Weyl nodes, $|\mathbf{M}^{\text{orb}}| \approx 4.68 \times 10^{-2}\text{A}/\text{m}$. Moreover, Weyl nodes are not mandatory, and the converse vortical effects can also occur in a chiral semimetal such as CoSi⁷⁴⁻⁷⁶.

VII. Summary

We employed the chiral kinematic theory for investigating the influence of space-time dependent velocity fields on electron fluids. Through analysis of the LDC, we explore the orbital magnetization response, that we dub the converse vortical effect, induced by the velocity field. By applying the Kubo formula, we calculate the converse vortical effect under different limits. Our study reveals that the magnetic susceptibility in the static limit, which encompasses both clean and disordered systems, and in the uniform limit of disordered systems, is determined by the orbital moment on the Fermi surface and the Berry curvature of occupied bands. These findings are in agreement with the predictions derived from chiral kinematic theories. However, in the uniform limit of clean systems, the susceptibility is solely determined by the Berry curvature of occupied bands. This research provides valuable insights into the behavior of electron fluids under space-time-dependent velocity fields, shedding light on the intricate relationship between the velocity field and electron properties. Our results contribute to advancing the understanding of fundamental physical phenomena and offer opportunities for exploring new applications in electron fluid systems.

Acknowledgments

We acknowledge support from the Department of Energy grant no. DE-SC0022264.

-
- ¹ M Zahid Hasan and Charles L Kane. Colloquium: topological insulators. *Reviews of modern physics*, 82(4):3045, 2010.
- ² Xiao-Liang Qi and Shou-Cheng Zhang. Topological insulators and superconductors. *Reviews of Modern Physics*, 83(4):1057, 2011.
- ³ Tsutomu Yanagida. Horizontal symmetry and masses of neutrinos. *Progress of Theoretical Physics*, 64(3):1103–1105, 1980.
- ⁴ Graciela B Gelmini and Marco Roncadelli. Left-handed neutrino mass scale and spontaneously broken lepton number. *Physics Letters B*, 99(5):411–415, 1981.
- ⁵ Tsung-Dao Lee and Chen-Ning Yang. Question of parity conservation in weak interactions. *Physical Review*, 104(1):254, 1956.
- ⁶ Chien-Shiung Wu, Ernest Ambler, Raymond W Hayward, Dale D Hoppes, and Ralph Percy Hudson. Experimental test of parity conservation in beta decay. *Physical review*, 105(4):1413, 1957.
- ⁷ Alexander Vilenkin. Macroscopic parity-violating effects: Neutrino fluxes from rotating black holes and in rotating thermal radiation. *Physical Review D*, 20(8):1807, 1979.
- ⁸ Naoki Yamamoto. Chiral transport of neutrinos in supernovae: Neutrino-induced fluid helicity and helical plasma instability. *Physical Review D*, 93(6):065017, 2016.
- ⁹ G Yu Prokhorov, OV Teryaev, and VI Zakharov. Chiral vortical effect: Black-hole versus flat-space derivation. *Physical Review D*, 102(12):121702, 2020.
- ¹⁰ Antonino Flachi and Kenji Fukushima. Chiral vortical effect with finite rotation, temperature, and curvature. *Physical Review D*, 98(9):096011, 2018.
- ¹¹ Stephon Alexander, Evan McDonough, and David N Spergel. Chiral gravitational waves and baryon superfluid dark matter. *Journal of Cosmology and Astroparticle Physics*, 2018(05):003, 2018.
- ¹² Luca Di Luzio, Guido Martinelli, and Gioacchino Piazza. Breakdown of chiral perturbation theory for the axion hot dark matter bound. *Physical review letters*, 126(24):241801, 2021.
- ¹³ Francesca Chadha-Day, John Ellis, and David JE Marsh. Axion dark matter: What is it and why now? *Science advances*, 8(8):eabj3618, 2022.
- ¹⁴ NP Armitage, EJ Mele, and Ashvin Vishwanath. Weyl and dirac semimetals in three-dimensional solids. *Reviews of Modern Physics*, 90(1):015001, 2018.
- ¹⁵ Pavan Hosur and Xiaoliang Qi. Recent developments in transport phenomena in weyl semimetals. *Comptes Rendus Physique*, 14(9-10):857–870, 2013.
- ¹⁶ Xiangang Wan, Ari M Turner, Ashvin Vishwanath, and Sergey Y Savrasov. Topological semimetal and fermi-arc surface states in the electronic structure of pyrochlore iridates. *Physical Review B*, 83(20):205101, 2011.
- ¹⁷ AA Burkov and Leon Balents. Weyl semimetal in a topological insulator multilayer. *Physical review letters*, 107(12):127205, 2011.
- ¹⁸ BQ Lv, HM Weng, BB Fu, X Ps Wang, Hu Miao, Junzhang Ma, P Richard, XC Huang, LX Zhao, GF Chen, et al. Experimental discovery of weyl semimetal taas. *Physical Review X*, 5(3):031013, 2015.
- ¹⁹ Alexey A Soluyanov, Dominik Gresch, Zhijun Wang, Quan-Sheng Wu, Matthias Troyer, Xi Dai, and B Andrei Bernevig. Type-ii weyl semimetals. *Nature*, 527(7579):495–498, 2015.
- ²⁰ Hongming Weng, Chen Fang, Zhong Fang, B Andrei Bernevig, and Xi Dai. Weyl semimetal phase in noncentrosymmetric transition-metal monophosphides. *Physical Review X*, 5(1):011029, 2015.
- ²¹ Su-Yang Xu, Ilya Belopolski, Nasser Alidoust, Madhab Neupane, Guang Bian, Chenglong Zhang, Raman Sankar, Guoqing Chang, Zhujun Yuan, Chi-Cheng Lee, et al. Discovery of a weyl fermion semimetal and topological fermi arcs. *Science*, 349(6248):613–617, 2015.
- ²² AA Zyuzin and AA Burkov. Topological response in weyl semimetals and the chiral anomaly. *Physical Review B*, 86(11):115133, 2012.
- ²³ Qiang Li, Dmitri E Kharzeev, Cheng Zhang, Yuan Huang, I Pletikosić, AV Fedorov, RD Zhong, JA Schneeloch, GD Gu, and T Valla. Chiral magnetic effect in zrte 5. *Nature Physics*, 12(6):550–554, 2016.
- ²⁴ Jing Ma and DA Pesin. Chiral magnetic effect and natural optical activity in metals with or without weyl points. *Physical Review B*, 92(23):235205, 2015.
- ²⁵ Ze-Min Huang, Jianhui Zhou, and Shun-Qing Shen. Topological responses from chiral anomaly in multi-weyl semimetals. *Physical Review B*, 96(8):085201, 2017.
- ²⁶ NP Ong and Sihang Liang. Experimental signatures of the chiral anomaly in dirac–weyl semimetals. *Nature Reviews Physics*, 3(6):394–404, 2021.
- ²⁷ Shuang Jia, Su-Yang Xu, and M Zahid Hasan. Weyl semimetals, fermi arcs and chiral anomalies. *Nature materials*, 15(11):1140–1144, 2016.
- ²⁸ Stephen L Adler. Axial-vector vertex in spinor electrodynamics. *Physical Review*, 177(5):2426, 1969.
- ²⁹ Bruno Zumino, Wu Yong-Shi, and Anthony Zee. Chiral anomalies, higher dimensions, and differential geometry. *Nuclear Physics B*, 239(2):477–507, 1984.
- ³⁰ Anton Yu Alekseev, Vadim V Cheianov, and Jürg Fröhlich. Universality of transport properties in equilibrium, the goldstone theorem, and chiral anomaly. *Physical review letters*, 81(16):3503, 1998.
- ³¹ Cheng-Long Zhang, Su-Yang Xu, Ilya Belopolski, Zhujun Yuan, Ziquan Lin, Bingbing Tong, Guang Bian, Nasser Alidoust, Chi-Cheng Lee, Shin-Ming Huang, et al. Signatures of the adler–bell–jackiw chiral anomaly in a weyl fermion semimetal. *Nature communications*, 7(1):1–9, 2016.
- ³² Niklas Mueller and Raju Venugopalan. Chiral anomaly, berry phase, and chiral kinetic theory from worldlines in quantum field theory. *Physical Review D*, 97(5):051901, 2018.
- ³³ Colin Rylands, Alireza Parhizkar, Anton A Burkov, and Victor Galitski. Chiral anomaly in interacting condensed matter systems. *Physical Review Letters*, 126(18):185303, 2021.

- 2021.
- ³⁴ EV Gorbar, VA Miransky, and IA Shovkovy. Chiral anomaly, dimensional reduction, and magnetoresistivity of weyl and dirac semimetals. Physical Review B, 89(8):085126, 2014.
- ³⁵ Andrew C Potter, Itamar Kimchi, and Ashvin Vishwanath. Quantum oscillations from surface fermi arcs in weyl and dirac semimetals. Nature communications, 5(1):5161, 2014.
- ³⁶ Jun Xiong, Satya K Kushwaha, Tian Liang, Jason W Krizan, Max Hirschberger, Wudi Wang, Robert Joseph Cava, and Nai Phuan Ong. Evidence for the chiral anomaly in the dirac semimetal na3bi. Science, 350(6259):413–416, 2015.
- ³⁷ Adolfo G Grushin, Jörn WF Venderbos, Ashvin Vishwanath, and Roni Ilan. Inhomogeneous weyl and dirac semimetals: Transport in axial magnetic fields and fermi arc surface states from pseudo-landau levels. Physical Review X, 6(4):041046, 2016.
- ³⁸ AA Burkov. Topological semimetals. Nature materials, 15(11):1145–1148, 2016.
- ³⁹ Tian Liang, Jingjing Lin, Quinn Gibson, Tong Gao, Max Hirschberger, Minhao Liu, Robert Joseph Cava, and Nai Phuan Ong. Anomalous nernst effect in the dirac semimetal cd 3 as 2. Physical review letters, 118(13):136601, 2017.
- ⁴⁰ MA Stephanov and Yi Yin. Chiral kinetic theory. Physical review letters, 109(16):162001, 2012.
- ⁴¹ Jing-Yuan Chen, Dam T Son, Mikhail A Stephanov, Ho-Ung Yee, and Yi Yin. Lorentz invariance in chiral kinetic theory. Physical Review Letters, 113(18):182302, 2014.
- ⁴² Gökçe Başar, Dmitri E Kharzeev, and Ho-Ung Yee. Triangle anomaly in weyl semimetals. Physical Review B, 89(3):035142, 2014.
- ⁴³ Karl Landsteiner. Anomalous transport of weyl fermions in weyl semimetals. Physical Review B, 89(7):075124, 2014.
- ⁴⁴ Atsuo Shitade, Kazuya Mameda, and Tomoya Hayata. Chiral vortical effect in relativistic and nonrelativistic systems. Physical Review B, 102(20):205201, 2020.
- ⁴⁵ Swadeepan Nanda and Pavan Hosur. Vortical effects in chiral band structures. Physical Review B, 107(20):205107, 2023.
- ⁴⁶ Dam Thanh Son and Naoki Yamamoto. Berry curvature, triangle anomalies, and the chiral magnetic effect in fermi liquids. Physical review letters, 109(18):181602, 2012.
- ⁴⁷ DT Son and BZ Spivak. Chiral anomaly and classical negative magnetoresistance of weyl metals. Physical Review B, 88(10):104412, 2013.
- ⁴⁸ Dam Thanh Son and Naoki Yamamoto. Kinetic theory with berry curvature from quantum field theories. Physical review D, 87(8):085016, 2013.
- ⁴⁹ AA Burkov. Chiral anomaly and transport in weyl metals. Journal of Physics: Condensed Matter, 27(11):113201, 2015.
- ⁵⁰ Yu-Chen Liu, Lan-Lan Gao, Kazuya Mameda, and Xu-Guang Huang. Chiral kinetic theory in curved spacetime. Physical Review D, 99(8):085014, 2019.
- ⁵¹ DE Kharzeev, JF Liao, SA Voloshin, and G Wang. Chiral magnetic and vortical effects in high energy nuclear collisions a status report. Progress in Particle and Nuclear Physics, 88:1–28, 2016.
- ⁵² Jiunn-Wei Chen, Takeaki Ishii, Shi Pu, and Naoki Yamamoto. Nonlinear chiral transport phenomena. Physical Review D, 93(12):125023, 2016.
- ⁵³ Yoshimasa Hidaka, Shi Pu, and Di-Lun Yang. Nonlinear responses of chiral fluids from kinetic theory. Physical Review D, 97(1):016004, 2018.
- ⁵⁴ Kazuya Mameda. Nonlinear chiral kinetic theory. Physical Review D, 108(1):016001, 2023.
- ⁵⁵ Ömer F Dayi and Eda Kilinçarslan. Quantum kinetic equation in the rotating frame and chiral kinetic theory. Physical Review D, 98(8):081701, 2018.
- ⁵⁶ Ömer F Dayi and Eda Kilinçarslan. Quantum kinetic equation for fluids of spin-1/2 fermions. Journal of High Energy Physics, 2021(11):1–30, 2021.
- ⁵⁷ Riki Toshio, Kazuaki Takasan, and Norio Kawakami. Anomalous hydrodynamic transport in interacting non-centrosymmetric metals. Physical Review Research, 2(3):032021, 2020.
- ⁵⁸ Nigel R Cooper. Rapidly rotating atomic gases. Advances in Physics, 57(6):539–616, 2008.
- ⁵⁹ Y-J Lin, Rob L Compton, Karina Jiménez-García, James V Porto, and Ian B Spielman. Synthetic magnetic fields for ultracold neutral atoms. Nature, 462(7273):628–632, 2009.
- ⁶⁰ Alexander L Fetter. Rotating trapped bose-einstein condensates. Reviews of Modern Physics, 81(2):647, 2009.
- ⁶¹ Nathan Goldman, G Juzeliūnas, Patrik Öhberg, and Ian B Spielman. Light-induced gauge fields for ultracold atoms. Reports on Progress in Physics, 77(12):126401, 2014.
- ⁶² David Bohm. Note on a theorem of bloch concerning possible causes of superconductivity. Physical Review, 75(3):502, 1949.
- ⁶³ Naoki Yamamoto. Generalized bloch theorem and chiral transport phenomena. Physical Review D, 92(8):085011, 2015.
- ⁶⁴ Shudan Zhong, Joel E Moore, and Ivo Souza. Gyrotropic magnetic effect and the magnetic moment on the fermi surface. Physical review letters, 116(7):077201, 2016.
- ⁶⁵ ZV Khaidukov, VP Kirilin, and AV Sadofyev. Chiral vortical effect in fermi liquid. Physics Letters B, 717(4-5):447–449, 2012.
- ⁶⁶ VP Kirilin, AV Sadofyev, and VI Zakharov. Chiral vortical effect in superfluid. Physical Review D, 86(2):025021, 2012.
- ⁶⁷ Artur Avkhadiev and Andrey V Sadofyev. Chiral vortical effect for bosons. Physical Review D, 96(4):045015, 2017.
- ⁶⁸ Ruslan Abramchuk, ZV Khaidukov, and MA Zubkov. Anatomy of the chiral vortical effect. Physical Review D, 98(7):076013, 2018.
- ⁶⁹ Jian-Hua Gao, Jin-Yi Pang, and Qun Wang. Chiral vortical effect in wigner function approach. Physical Review D, 100(1):016008, 2019.
- ⁷⁰ Ganesh Sundaram and Qian Niu. Wave-packet dynamics in slowly perturbed crystals: Gradient corrections and berry-phase effects. Physical Review B, 59(23):14915, 1999.
- ⁷¹ Liang Dong, Cong Xiao, Bangguo Xiong, and Qian Niu. Berry phase effects in dipole density and the mott relation. Physical Review Letters, 124(6):066601, 2020.
- ⁷² Yang Gao. Implication of berry phase in nonlinear transport phenomena. Low. Temp. Phys. Lett. 41, 0241 (2019).
- ⁷³ Masao Ogata. Theory of magnetization in bloch electron systems. Journal of the Physical Society of Japan, 86(4):044713, 2017.
- ⁷⁴ Zhicheng Rao, Hang Li, Tiantian Zhang, Shangjie Tian, Chenghe Li, Binbin Fu, Cenyao Tang, Le Wang, Zhilin Li, Wenhui Fan, et al. Observation of unconventional chiral fermions with long fermi arcs in cosi. Nature, 567(7749):496–499, 2019.

- ⁷⁵ Daichi Takane, Zhiwei Wang, Seigo Souma, Kosuke Nakayama, Takechika Nakamura, Hikaru Oinuma, Yuki Nakata, Hideaki Iwasawa, Cephise Cacho, Timur Kim, et al. Observation of chiral fermions with a large topological charge and associated fermi-arc surface states in *cosi*. Physical review letters, 122(7):076402, 2019.
- ⁷⁶ Bing Xu, Zhenyao Fang, Miguel-Ángel Sánchez-Martínez, Jorn WF Venderbos, Zhuoliang Ni, Tian Qiu, Kaustuv Manna, Kefeng Wang, Johnpierre Paglione, Christian Bernhard, et al. Optical signatures of multifold fermions in the chiral topological semimetal *cosi*. Proceedings of the National Academy of Sciences, 117(44):27104–27110, 2020.
- ⁷⁷ Jeeva Anandan and Jun Suzuki. Quantum mechanics in a rotating frame. In Relativity in rotating frames: relativistic physics in rotating reference frames, pages 361–370. Springer, 2004.
- ⁷⁸ Di Xiao, Ming-Che Chang, and Qian Niu. Berry phase effects on electronic properties. Reviews of modern physics, 82(3):1959, 2010.
- ⁷⁹ Alex Kamenev. Field theory of non-equilibrium systems. Cambridge University Press, 2023.

Appendix A: Perturbation induced by velocity field

In this section, we derive the perturbation term $-\hat{\mathbf{k}} \cdot \mathbf{v}(\mathbf{r}, t)$ induced by a space-time dependent velocity field $\mathbf{v}(\mathbf{r}, t)$. To achieve this, we consider electrons on a lattice governed by a Bloch Hamiltonian $H_0(\hat{\mathbf{k}})$. Under the influence of a space-time dependent velocity field, the position of the electrons is shifted by a small space-time dependent displacement $\mathbf{x}(\mathbf{r}, t)$ relative to the lattice background. Thus, in a reference frame moving with the electron fluid, the wave function evolves in time as

$$\psi(\mathbf{r}, t) = \hat{T}[e^{i \int_{\mathbf{x}(0)}^{\mathbf{x}(t)} \hat{\mathbf{k}} \cdot d\mathbf{x}(\mathbf{r}, \tau) - itH_0(\hat{\mathbf{k}})}] \psi(\mathbf{r}, 0) = \hat{T}[e^{i \int_0^t d\tau \hat{\mathbf{k}} \cdot \frac{\partial \mathbf{x}(\mathbf{r}, \tau)}{\partial \tau} - itH_0(\hat{\mathbf{k}})}] \psi(\mathbf{r}, 0), \quad (\text{A1})$$

where \hat{T} denotes time ordering and $\hat{\mathbf{k}}$ is the momentum operator that generates spatial translations. By factoring out the "unperturbed time-dependence", we can derive the perturbation term by defining $\psi_I(\mathbf{r}, t) = e^{itH_0(\hat{\mathbf{k}})} \psi(\mathbf{r}, t)$, which leads to:

$$i\partial_t \psi_I(\mathbf{r}, t) = -\hat{\mathbf{k}} \cdot \partial_t \mathbf{x}(\mathbf{r}, t) \psi_I(\mathbf{r}, t) \equiv -\hat{\mathbf{k}} \cdot \mathbf{v}(\mathbf{r}, t) \psi_I(\mathbf{r}, t). \quad (\text{A2})$$

The above equation indicates that $\psi_I(\mathbf{r}, t)$ behaves like a wave function in the Interaction Picture with an unperturbed Hamiltonian $H_0(\hat{\mathbf{k}})$ and perturbation $-\hat{\mathbf{k}} \cdot \mathbf{v}(\mathbf{r}, t)$. Therefore, the total Hamiltonian in the moving frame can be expressed as:

$$H(\hat{\mathbf{k}}, \mathbf{r}, t) = H_0(\hat{\mathbf{k}}) - \hat{\mathbf{k}} \cdot \mathbf{v}(\mathbf{r}, t). \quad (\text{A3})$$

The perturbation term $-\hat{\mathbf{k}} \cdot \mathbf{v}$ is naturally associated with the Galilean boost. For instance, for electrons described by the Hamiltonian $H_0 = \frac{\hat{\mathbf{k}}^2}{2m}$, the momentum $\hat{\mathbf{k}}$ transforms as $\hat{\mathbf{k}} \rightarrow \hat{\mathbf{k}} - m\mathbf{v}$, and the Hamiltonian $H_0 = \frac{\hat{\mathbf{k}}^2}{2m}$ is modified to $H = \frac{(\hat{\mathbf{k}} - m\mathbf{v})^2}{2m} = \frac{\hat{\mathbf{k}}^2}{2m} - \hat{\mathbf{k}} \cdot \mathbf{v} + O(\mathbf{v}^2)$ ⁷⁷. However, the derivation of the perturbation term $-\hat{\mathbf{k}} \cdot \mathbf{v}$ in Eq. (A3) is more general and not restricted to this specific context. For instance, for massless Weyl fermions, the transformation $\hat{\mathbf{k}} \rightarrow \hat{\mathbf{k}} - m\mathbf{v}$ fails because $m = 0$, but our results in Eq. (A3) remain valid. Indeed, the perturbation $-\hat{\mathbf{k}} \cdot \mathbf{v}$ is routinely employed in the literature to describe Weyl fermions moving with constant linear velocity⁴¹. Eq. (A3) merely generalizes it to smooth space-time dependent velocities.

Appendix B: Equations of semiclassical motion

In this section, we explore the semiclassical equation of motion using the semiclassical wave-packet dynamics method. First, we review the equation of motion for electrons under a general space-time dependent perturbation. Detailed discussions can be found in Ref.⁷⁰. Secondly, we apply these equations of motion (EM) to a system under a space-time dependent velocity field and derive the density of orbital magnetization.

1. Semiclassical wave-packet dynamics

Consider a system under a set of general space-time dependent perturbations with the following Hamiltonian:

$$H \equiv H(\hat{\mathbf{k}}, \mathbf{r}; \theta(\mathbf{r}, t), t), \quad (\text{B1})$$

where the first \mathbf{r} represents the fast-changing part, and the $\theta(\mathbf{r}, t)$ represents the set of slowly changing perturbations. After expanding the slowly changing part of the Hamiltonian around wave packet center \mathbf{r}_c , Ref.⁷⁰ obtained

$$H = H_c \left(\hat{\mathbf{k}}, \mathbf{r}; \theta(\mathbf{r}_c, t), t \right) + H_1 \left(\hat{\mathbf{k}}, \mathbf{r}; \mathbf{r}_c, t \right) + \dots \quad (\text{B2})$$

In general, the local Hamiltonian H_c has eigenvalue $\epsilon_n(\mathbf{p}, \mathbf{r}_c, t)$ and eigenstate $e^{i\mathbf{p}\cdot\mathbf{r}}|u_n(\mathbf{p}, \mathbf{r}_c, t)\rangle$. To obtain the equations of motion, Ref.⁷⁰ first derive the Lagrangian $L \equiv \langle \Psi | (i\partial_t - H) | \Psi \rangle$, where the wave packet wave function is constructed as a superposition of Bloch states from band n

$$|\Psi\rangle = \int d\mathbf{p} a(\mathbf{p}) e^{i\mathbf{p}\cdot\mathbf{r}} |u_n(\mathbf{p}, \mathbf{r}_c, t)\rangle. \quad (\text{B3})$$

The normalization of $|\Psi\rangle$ indicates $\int d\mathbf{p} |a(\mathbf{p})| = 1$, and the magnitude of $a(\mathbf{p}) = |a(\mathbf{p})| e^{-i\gamma(\mathbf{p}, \mathbf{r}, t)}$ satisfies $|a(\mathbf{p})|^2 \approx \delta(\mathbf{p} - \mathbf{k}_c)$, where $\mathbf{k}_c = \langle \Psi | \hat{\mathbf{k}} | \Psi \rangle$ is the center of mass of momentum of the wave packet. The center of mass position \mathbf{r}_c of the wave packet is determined in the following way

$$\mathbf{r}_c = \langle \Psi | \mathbf{r} | \Psi \rangle = \int d\mathbf{p} d\mathbf{q} a^*(\mathbf{p}) a(\mathbf{q}) \langle u_n(\mathbf{p}, \mathbf{r}_c, t) | (i\partial_{\mathbf{p}} e^{-i\mathbf{p}\cdot\mathbf{r}}) e^{i\mathbf{q}\cdot\mathbf{r}} | u_n(\mathbf{q}, \mathbf{r}_c, t) \rangle = \partial_{\mathbf{k}_c} \gamma(\mathbf{k}_c, \mathbf{r}_c, t) + \mathcal{A}_n(\mathbf{k}_c, \mathbf{r}_c, t), \quad (\text{B4})$$

where $\gamma(\mathbf{k}_c, \mathbf{r}_c, t) = -\arg a(\mathbf{k}_c)$, and $\mathcal{A}_n(\mathbf{k}_c, \mathbf{r}_c, t)$ is the Berry connection in band n . The energy part can be evaluated:

$$\langle \Psi | H_c | \Psi \rangle = \epsilon_n(\mathbf{k}_c, \mathbf{r}_c, t), \quad (\text{B5})$$

$$\langle \Psi | H_1 | \Psi \rangle = \text{Im} \langle \partial_{p_i} u_n | \epsilon - H_c | \partial_{\theta} u_n \rangle \cdot \partial_{r_i} \theta, \quad (\text{B6})$$

Additionally, the dynamic part takes the following form

$$\langle \Psi | i\partial_t | \Psi \rangle = \langle u_n | i\partial_t | u_n \rangle + \dot{\mathbf{r}}_c \cdot \langle u_n | i\partial_{\mathbf{r}_c} | u_n \rangle + \dot{\mathbf{k}}_c \cdot \langle u_n | i\partial_{\mathbf{k}_c} | u_n \rangle - \mathbf{r}_c \cdot \dot{\mathbf{k}}_c, \quad (\text{B7})$$

up to a global time derivative. Therefore, the Lagrangian takes the form

$$L = \langle u_n | i\partial_t | u_n \rangle + \dot{\mathbf{r}}_c \cdot \langle u_n | i\partial_{\mathbf{r}_c} | u_n \rangle + \dot{\mathbf{k}}_c \cdot \langle u_n | i\partial_{\mathbf{k}_c} | u_n \rangle - \mathbf{r}_c \cdot \dot{\mathbf{k}}_c - E_n(\mathbf{k}_c, \mathbf{r}_c, t), \quad (\text{B8})$$

where the energy

$$E_n(\mathbf{k}_c, \mathbf{r}_c, t) = \epsilon_n(\mathbf{k}_c, \mathbf{r}_c, t) + \text{Im} \langle \partial_{p_i} u_n | \epsilon - \hat{H} | \partial_{\theta} u_n \rangle \cdot \partial_{r_i} \theta \equiv E_n. \quad (\text{B9})$$

Using the Lagrangian, one can derive the EM using the Euler-Lagrange equations. The EM is given by

$$\begin{cases} \dot{\mathbf{r}}_c = \partial_{\mathbf{k}_c} E_n - \Omega_{\mathbf{k}_c t} - \Omega_{\mathbf{k}_c \mathbf{r}_c} \cdot \dot{\mathbf{r}}_c - \Omega_{\mathbf{k}_c \mathbf{k}_c} \cdot \dot{\mathbf{k}}_c, \\ \dot{\mathbf{k}}_c = -\partial_{\mathbf{r}_c} E_n + \Omega_{\mathbf{r}_c t} + \Omega_{\mathbf{r}_c \mathbf{r}_c} \cdot \dot{\mathbf{r}}_c + \Omega_{\mathbf{r}_c \mathbf{k}_c} \cdot \dot{\mathbf{k}}_c. \end{cases} \quad (\text{B10})$$

where $\Omega_{\alpha\beta}^{ij} = \partial_{\alpha_i} \mathcal{A}_{\beta}^j - \partial_{\beta_j} \mathcal{A}_{\alpha}^i$ is the Berry curvature in generalized space spanned by $\{\mathbf{r}_c, \mathbf{k}_c, t\}$, and $\mathcal{A}_{\alpha}^j \equiv \langle u_n | i\partial_{\alpha_j} | u_n \rangle$ denotes the Berry connection. In the continuum limit, the EM are obtained by reducing the momentum \mathbf{k}_c in Eq. B10 to the continuum momentum \mathbf{k} .

2. LDC and orbital magnetization

After reviewing the necessary techniques and concepts in wave packet dynamics and EM. We now derive the local density of current (LDC) using the generic method proposed in Ref.⁷¹, and extract the orbital magnetization from the LDC. To obtain the LDC, we introduce an auxiliary coupling term $-\hat{\mathbf{J}} \cdot \mathbf{K}(\mathbf{r}, t)$ ($\mathbf{K}(\mathbf{r}, t)$ is the auxiliary momentum field and $\hat{\mathbf{J}} = \nabla_{\hat{\mathbf{k}}} H_0$ is the velocity or current operator) to the Hamiltonian. In fact, the LDC is obtained in the limit where $\mathbf{K}(\mathbf{r}, t) = 0$. The total system is described by the following Hamiltonian

$$H \left(\hat{\mathbf{k}}, \mathbf{r}; \mathbf{r}, t \right) = H_0 \left(\hat{\mathbf{k}}, \mathbf{r} \right) - \hat{\mathbf{k}} \cdot \mathbf{v}(\mathbf{r}, t) - \hat{\mathbf{J}} \cdot \mathbf{K}(\mathbf{r}, t), \quad (\text{B11})$$

The set of slowly varying perturbations $\theta(\mathbf{r}, t)$ in equation (B1) now takes the form $\mathbf{K}(\mathbf{r}, t), \mathbf{v}(\mathbf{r}, t)$. The zero order local Hamiltonian has the following form

$$H_c = H_0 \left(\hat{\mathbf{k}}, \mathbf{r} \right) - \hat{\mathbf{k}} \cdot \mathbf{v}(\mathbf{r}_c, t) - \hat{\mathbf{J}} \cdot \mathbf{K}(\mathbf{r}_c, t) \equiv \hat{H}. \quad (\text{B12})$$

In the derivation of the LDC, we need the EM for the Hamiltonian B11. Therefore, we first obtain the EM by applying the semiclassical wave-packet dynamics method, as discussed in the previous subsection, to the Hamiltonian B11. The wave packet is constructed as

$$|\Psi\rangle = \int d^3\mathbf{k} a(\mathbf{k}) e^{i\mathbf{k}\cdot\mathbf{x}} |u_n(\mathbf{k}, \mathbf{v}, \mathbf{K}, t)\rangle, \quad (\text{B13})$$

where \mathbf{k} is the eigenvalue of the momentum operator $\hat{\mathbf{k}}$, and $|u_n(\mathbf{k}, \mathbf{v}(\mathbf{r}_c, t), \mathbf{K}(\mathbf{r}_c, t), t)\rangle$ is the eigenstate of the local Hamiltonian H_c , with the corresponding eigenvalue is $\epsilon_n(\mathbf{v}(\mathbf{r}_c, t), \mathbf{K}(\mathbf{r}_c, t))$. The equations (B5) and (B6) are transformed into

$$\langle\Psi|\hat{H}|\Psi\rangle = \epsilon_n(\mathbf{v}(\mathbf{r}_c, t), \mathbf{K}(\mathbf{r}_c, t)), \quad (\text{B14})$$

$$\delta\epsilon_n = \text{Im}\langle\partial_{k_i}u_n|\epsilon - \hat{H}|\partial_{\mathbf{v}}u_n\rangle \cdot \partial_{r_i}\mathbf{v} + \text{Im}\langle\partial_{k_i}u_n|\epsilon - \hat{H}|\partial_{\mathbf{K}}u_n\rangle \cdot \partial_{r_i}\mathbf{K}, \quad (\text{B15})$$

The dynamic part takes the same form as Eq. (B7), and the Lagrangian reads

$$L = \mathcal{A}_t + \dot{\mathbf{r}}_c \cdot \mathcal{A}_{\mathbf{r}_c} + \dot{\mathbf{k}}_c \cdot \mathcal{A}_{\mathbf{k}_c} + \dot{\mathbf{k}}_c \cdot \mathbf{r}_c - E, \quad (\text{B16})$$

where the $\mathcal{A}_i = \langle u_n | i\partial_i | u_n \rangle$ for $i \in \{\mathbf{k}_c, \mathbf{r}_c, t\}$ are Berry connections, and the energy is given by

$$E = \epsilon + \delta\epsilon. \quad (\text{B17})$$

To simplify the notation, we have omitted the center position label c and the band index n , and will continue to do so henceforth. The EM is modified to

$$\begin{cases} \dot{\mathbf{r}} = \partial_{\mathbf{k}}E - \Omega_{\mathbf{k}t} - \Omega_{\mathbf{k}\mathbf{r}} \cdot \dot{\mathbf{r}} - \Omega_{\mathbf{k}\mathbf{k}} \cdot \dot{\mathbf{k}}, \\ \dot{\mathbf{k}} = -\partial_{\mathbf{r}}E + \Omega_{\mathbf{r}t} + \Omega_{\mathbf{r}\mathbf{r}} \cdot \dot{\mathbf{r}} + \Omega_{\mathbf{r}\mathbf{k}} \cdot \dot{\mathbf{k}}. \end{cases} \quad (\text{B18})$$

After deriving the necessary EM, we proceed to derive the LDC. The LDC is expressed as follows (see Eq. (10) in the supplementary material of Ref.⁷¹):

$$\rho_{\text{loc}}^{\mathbf{J}} = \lim_{\mathbf{K} \rightarrow 0} \left\{ - \int d\mathbf{k} Df \left[\frac{\partial E}{\partial \mathbf{K}} - \Omega_{\mathbf{K}\mathcal{T}} \right] - \nabla \cdot \int d\mathbf{k} Df \text{Im} \langle \partial_{\mathbf{k}}u_n | \epsilon - \hat{H} | \partial_{\mathbf{K}}u_n \rangle \right\} \quad (\text{B19})$$

where $\Omega_{\mathbf{K}\mathcal{T}} = \dot{\mathbf{k}} \cdot \Omega_{\mathbf{K}\mathbf{k}} + \dot{\mathbf{r}} \cdot \Omega_{\mathbf{K}\mathbf{r}} + \Omega_{\mathbf{K}t}$, the local equilibrium distribution $f = (1 + e^{\beta\epsilon(\mathbf{v}, \mathbf{K})})^{-1}$, and $D \equiv 1 + \Omega_{k_i r_i}$ serves as the phase space measure.

In the second term of $\rho_{\text{loc}}^{\mathbf{J}}$, it suffices to set $D = 1$, as $\rho_{\text{loc}}^{\mathbf{J}}$ is considered only up to first order⁷¹. Additionally, the second term, being the divergence of a vector, clearly contributes to the orbital magnetization based on the definition of LDC in Ref.⁷¹. However, for the first term in $\rho_{\text{loc}}^{\mathbf{J}}$, further calculations are necessary to clarify how it contributes to the orbital magnetization. We now provide these details.

Using the EM (B18), the first term within the the $\{\}$ of $\rho_{\text{loc}}^{\mathbf{J}}$ is given by

$$\begin{aligned} & - \int d\mathbf{k} Df \left[\frac{\partial E}{\partial \mathbf{K}} - \Omega_{\mathbf{K}\mathcal{T}} \right] \quad (\text{B20}) \\ &= - \int d\mathbf{k} f \left[\frac{\partial E}{\partial \mathbf{K}} + \Omega_{\mathbf{K}k_i} \partial_{r_i} \epsilon - \Omega_{\mathbf{K}r_i} \partial_{k_i} \epsilon - \Omega_{\mathbf{K}t} + \Omega_{k_i r_i} \frac{\partial \epsilon}{\partial \mathbf{K}} \right] \\ &= - \int d\mathbf{k} \left[\frac{\partial g}{\partial \mathbf{K}} - f \Omega_{\mathbf{K}t} + \frac{\partial(\Omega_{k_i r_i} g)}{\partial \mathbf{K}} + \frac{\partial(\Omega_{\mathbf{K}k_i} g)}{\partial r_i} - g(\partial_{k_i} \Omega_{\mathbf{K}r_i} + \partial_{r_i} \Omega_{k_i \mathbf{K}} + \partial_{\mathbf{K}} \Omega_{r_i k_i}) \right], \quad (\text{B21}) \end{aligned}$$

where the function $g = -\frac{1}{\beta} \ln^{1+e^{-\beta\epsilon(\mathbf{v}, \mathbf{K})}}$ arises due to integration by parts. By applying the Bianchi identity $\partial_{k_i} \Omega_{\mathbf{K}r_i} + \partial_{r_i} \Omega_{k_i \mathbf{K}} + \partial_{\mathbf{K}} \Omega_{r_i k_i} = 0$, the above equation can be simplified as follows:

$$\begin{aligned} - \int d\mathbf{k} Df \left[\frac{\partial E}{\partial \mathbf{K}} - \Omega_{\mathbf{K}\mathcal{T}} \right] &= - \int d\mathbf{k} \left[\frac{\partial g}{\partial \mathbf{K}} - f \Omega_{\mathbf{K}t} + \frac{\partial(\Omega_{k_i r_i} g)}{\partial \mathbf{K}} + \frac{\partial(\Omega_{\mathbf{K}k_i} g)}{\partial r_i} \right] \\ &= - \partial_{\mathbf{K}} \int d\mathbf{k} (1 + \Omega_{k_i r_i}) g - \partial_{r_i} \int d\mathbf{k} \Omega_{\mathbf{K}k_i} g + \int d\mathbf{k} f \Omega_{\mathbf{K}t} \\ &= - \partial_{\mathbf{K}} \int d\mathbf{k} (1 + \Omega_{k_i r_i}) g + \nabla \cdot \int d\mathbf{k} \Omega_{\mathbf{k}\mathbf{K}} g + \int d\mathbf{k} f \Omega_{\mathbf{K}t}, \quad (\text{B22}) \end{aligned}$$

Since the vector potential \mathbf{K} is minimally coupled to the momentum in the Hamiltonian through $\mathbf{k} - \mathbf{K}$, the derivative with respect to \mathbf{K} can be replaced by the derivative with respect to \mathbf{k} . Note that the second term in the last equality of Eq. B22 is a total divergence of a vector; hence it will contribute to the orbital magnetization. By combining the first and second terms of Eq. (B19) and taking the limit $\mathbf{K} \rightarrow 0$, we derive the LDC as:

$$\begin{aligned} \rho_{\text{loc}}^{\mathbf{J}} &= -\partial_{\mathbf{k}} \int d\mathbf{k} (1 + \Omega_{k_i r_i}) g - \nabla \cdot \int d\mathbf{k} (-g \Omega_{\mathbf{k}\mathbf{k}} + f \text{Im} \langle \partial_{\mathbf{k}} u_n | \epsilon - \hat{H} | \partial_{\mathbf{k}} u_n \rangle) + \int d\mathbf{k} f \Omega_{\mathbf{k}t} \\ &= -\nabla \cdot \int d\mathbf{k} (-g \Omega_{\mathbf{k}\mathbf{k}} + f \text{Im} \langle \partial_{\mathbf{k}} u_n | \epsilon - \hat{H} | \partial_{\mathbf{k}} u_n \rangle) + \int d\mathbf{k} f \Omega_{\mathbf{k}t} \equiv -\partial_i M^{i\mathbf{J}} + \int d\mathbf{k} f \Omega_{\mathbf{k}t}, \end{aligned} \quad (\text{B23})$$

where the second equality holds because \mathbf{k} has already been integrated out.

From the LDC (Eq. B23), we can extract the orbital magnetization⁷¹

$$M^{iJ_j} = \int d\mathbf{k} (-g \Omega_{k_i k_j} + f \text{Im} \langle \partial_{k_i} u_n | \epsilon - \hat{H} | \partial_{k_j} u_n \rangle) \equiv M_{ij}, \quad (\text{B24})$$

Its vector form is given by

$$M_l^{\text{orb}} = \frac{\epsilon_{lij} M_{ij}}{2} = \int d\mathbf{k} \frac{1}{2} (-g \epsilon_{lij} \Omega_{k_i k_j} + f \epsilon_{lij} \text{Im} \langle \partial_{k_i} u_n | \epsilon - \hat{H} | \partial_{k_j} u_n \rangle) = \int d\mathbf{k} (f m_l^{\text{orb}} - g \Omega_l(\mathbf{k})), \quad (\text{B25})$$

where $\Omega_l(\mathbf{k})$ is the l^{th} component of the Berry curvature, and m_l^{orb} is the l^{th} component of the orbital magnetic moment. Notice that after taking the limit $\mathbf{K} \rightarrow 0$, the distribution functions f and g take the following form

$$\begin{cases} f = \frac{1}{1 + e^{\beta(\epsilon - \mathbf{k} \cdot \mathbf{v})}}, \\ g = -\frac{1}{\beta} \ln[1 + e^{-\beta(\epsilon - \mathbf{k} \cdot \mathbf{v})}]. \end{cases} \quad (\text{B26})$$

Ultimately, by accounting for the band index and combining the effects from each band, we can derive the formula for the density of orbital magnetization. This accounts for the cumulative effect of all individual bands, providing a complete representation of the orbital magnetization density in the system, which is now given by:

$$\mathbf{M}^{\text{orb}} = \sum_n \int d\mathbf{k} \{ f \mathbf{m}_n^{\text{orb}} + \frac{1}{\beta} \ln[1 + e^{-\beta(\epsilon_n - \mathbf{k} \cdot \mathbf{v})}] \boldsymbol{\Omega}_n \}, \quad (\text{B27})$$

Conversely, for a filled band, when using a gauge where \mathcal{A}_t is periodic in the Brillouin zone, the last term in Eq. (B23) can be written as:

$$\int d\mathbf{k} \Omega_{\mathbf{k}t} = -\partial_t \int d\mathbf{k} \mathcal{A}_{\mathbf{k}} = -\partial_t \mathbf{P}, \quad (\text{B28})$$

where \mathbf{P} denotes the polarization. As a result, this final term represents the current generated by the polarization.

Appendix C: Orbital magnetization of a parabolic band under a static velocity field

In this Appendix, we derive the EM for a parabolic band with Berry phases due to internal degrees of freedom using the analogy between the velocity field and the electromagnetic vector potential. We then obtain the orbital magnetization by varying the appropriate equilibrium free energy density.

1. Alternate derivation of the EM

Consider electrons described by a Bloch Hamiltonian $H_0(\mathbf{k})$, where a band near its bottom can be approximated by a parabolic dispersion with an effective mass m . Upon applying an external static velocity field, the effective Hamiltonian is modified as:

$$H(\mathbf{k}, \mathbf{r}) = \frac{\mathbf{k}^2}{2m} - \mathbf{k} \cdot \mathbf{v}(\mathbf{r}). \quad (\text{C1})$$

For sufficiently weak velocity fields compared to the typical group velocity, we can approximate the Hamiltonian as follows :

$$H \approx \frac{(\mathbf{k} - m\mathbf{v}(\mathbf{r}))^2}{2m}. \quad (\text{C2})$$

Noticing that this Hamiltonian is similar to the local Hamiltonian of electrons under magnetic fields in Refs.^{70,72,78}, with $\mathbf{v}(\mathbf{r}_c)$ a similar role to the magnetic vector potential $\mathbf{A}(\mathbf{r}_c)$, and the angular velocity $\mathcal{V} \equiv \frac{1}{2}\nabla \times \mathbf{v}$ can be identified as the magnetic field $\mathbf{B} = \nabla \times \mathbf{A}$. Given the aforementioned similarities between the velocity \mathbf{v} and the magnetic vector potential \mathbf{A} , and between the angular velocity \mathcal{V} and the magnetic field \mathbf{B} , we immediately obtain the Lagrangian for our model as:

$$L = \mathbf{k} \cdot \dot{\mathbf{r}} - \dot{\mathbf{r}} \cdot m\mathbf{v} + \dot{\mathbf{k}} \cdot \mathcal{A}(\mathbf{k}) - h(\mathbf{k}), \quad (\text{C3})$$

with the energy $h(\mathbf{k}) = \epsilon_n(\mathbf{k}) - 2m\mathcal{V} \cdot \mathbf{m}_n^{\text{orb}}$. The Eq. (C3) is similar to the Eq. (3.7) in Ref.⁷⁰. Plugging the Eq. (C3) into the Euler-Lagrange equations, one can obtain the EM as

$$\begin{cases} \dot{\mathbf{r}} = \partial_{\mathbf{k}} h - \dot{\mathbf{k}} \times \boldsymbol{\Omega}_n, \\ \dot{\mathbf{k}} = -\partial_{\mathbf{r}} h - \dot{\mathbf{r}} \times 2m\mathcal{V}, \end{cases} \quad (\text{C4})$$

where $\boldsymbol{\Omega}_n$ denotes the Berry curvature of the n th band. As expected, the above EM is similar to the EM for an electron under a magnetic field, such as Equation (3.8) in Ref.⁷⁰ and Equations (5.8a,b) in Ref.⁷⁸.

The Berry curvature in above EM implies that the \mathbf{r}, \mathbf{k} are not canonical coordinates. In reminder of this section, we investigate the impact of the equations of motion on the phase space spanned by noncanonical coordinates. In canonical coordinates, denoted as $\eta = (\mathbf{q}, \mathbf{p})$, the Hamilton equations can be expressed as $\dot{\eta}^\alpha \theta_{\alpha\beta} = \partial_\beta h$, where the antisymmetric matrix $\theta \equiv J = (0, 1; -1, 0)$ is known as the symplectic form⁷⁹. This establishes the foundation for understanding the dynamics in canonical coordinates.

For the equations of motion presented in Eq. (C4), the corresponding symplectic form exhibits a distinct structure. It can be expressed as:

$$\theta_{\alpha\beta} = \begin{pmatrix} \epsilon_{ijl} 2m\mathcal{V}^l & \delta_{ij} \\ -\delta_{ij} & -\epsilon_{ijl} \Omega_n^l \end{pmatrix} \quad (\text{C5})$$

Here, α and β represent elements from the set $\{\mathbf{r}, \mathbf{k}\}$, while i, j , and l take values from the set $\{x, y, z\}$. This modified symplectic form reveals new insights into the equations of motion in noncanonical coordinates. It highlights the influence of the antisymmetric matrix and the additional terms that arise due to the distinct structure of the symplectic form.

In the canonical coordinates $\eta = (\mathbf{q}, \mathbf{p})$, the phase-space volume element is given by $dV = d\mathbf{q}d\mathbf{p}$. However, when changing coordinates to noncanonical coordinates $\eta \rightarrow \zeta = (\mathbf{r}, \mathbf{k})$, the symplectic form undergoes a transformation. Specifically, $J_{\alpha\beta} \rightarrow \theta_{\alpha\beta} = \frac{\partial \eta^\sigma}{\partial \zeta^\alpha} \frac{\partial \eta^\gamma}{\partial \zeta^\beta} J_{\sigma\gamma}$. This transformation of the symplectic form leads to a corresponding transformation in the phase-space volume element.

The volume element in noncanonical coordinates is given by $dV = \sqrt{|\det \theta|} d\mathbf{r}d\mathbf{k} = (1 + 2m\boldsymbol{\Omega}_n \cdot \mathcal{V}) d\mathbf{r}d\mathbf{k}$. This expression elucidates the modification to the volume element due to the transformation and emphasizes the role of the additional terms involving the parameters $\boldsymbol{\Omega}_n$ and \mathcal{V} .

These results shed light on the structure of the symplectic form in noncanonical coordinates and its impact on the phase-space volume element. Understanding these transformations is vital for comprehending the dynamics and exploring various physical systems with different coordinate choices.

2. Free energy and orbital magnetization

In this part, we employ the modified phase-space volume, which in turn modifies the free energy density, to calculate the orbital magnetization response to the velocity field to linear order.

Consider a probability distribution function over the phase space volume, denoted as $n(\mathbf{r}, \mathbf{k}, \mathbf{t})(1 + 2\boldsymbol{\Omega}_n \cdot m\mathcal{V}) d\mathbf{r}d\mathbf{k}$. Under a Hamiltonian flow (without collisions), it evolves according to

$$\frac{\partial n}{\partial t} + \partial_{\mathbf{r}}(n\dot{\mathbf{r}}) + \partial_{\mathbf{k}}(n\dot{\mathbf{k}}) = -n \frac{d_t(2\boldsymbol{\Omega}_n \cdot m\mathcal{V})}{1 + 2\boldsymbol{\Omega}_n \cdot m\mathcal{V}}, \quad (\text{C6})$$

where $d_t(2\boldsymbol{\Omega}_n \cdot m\mathcal{V}) \equiv \partial_t(2\boldsymbol{\Omega}_n \cdot m\mathcal{V}) + \partial_{\mathbf{r}}(2\boldsymbol{\Omega}_n \cdot m\mathcal{V}) \cdot \dot{\mathbf{r}} + \partial_{\mathbf{k}}(2\boldsymbol{\Omega}_n \cdot m\mathcal{V}) \cdot \dot{\mathbf{k}}$. The Eq. (C6) does not have a form of the continuity relation, due to the presence of the right-hand side. This reflects the fact that $\int d\mathbf{r}d\mathbf{k}n(\mathbf{r}, \mathbf{k}, t)$ is not conserved.

However, the quantity $\int d\mathbf{r}d\mathbf{k}\tilde{n}(\mathbf{r}, \mathbf{k}, t) \equiv \int d\mathbf{r}d\mathbf{k}n(\mathbf{r}, \mathbf{k}, t)(1 + 2\boldsymbol{\Omega}_n \cdot m\boldsymbol{\mathcal{V}})$ remains conserved. Therefore, any observables should be expressed as $O_t = \int d\mathbf{r}d\mathbf{k}(1 + 2\boldsymbol{\Omega}_n \cdot m\boldsymbol{\mathcal{V}})n(\mathbf{r}, \mathbf{k}, t)O(\mathbf{r}, \mathbf{k}, t)$. Also, $\tilde{n}(\mathbf{r}, \mathbf{k}, t) \equiv (1 + 2\boldsymbol{\Omega}_n \cdot m\boldsymbol{\mathcal{V}})n(\mathbf{r}, \mathbf{k}, t)$ satisfies the continuity equation:

$$\frac{\partial \tilde{n}}{\partial t} + \dot{\mathbf{r}} \cdot \partial_{\mathbf{r}} \tilde{n} + \dot{\mathbf{k}} \cdot \partial_{\mathbf{k}} \tilde{n} = 0. \quad (\text{C7})$$

Similar to \mathbf{B} in the chiral kinetic theory, $\boldsymbol{\mathcal{V}}$ modifies the phase space measure in the free energy density:

$$F = -\frac{1}{\beta} \sum_n \int_{\mathbf{k}} (1 + 2\boldsymbol{\Omega}_n(\mathbf{k}) \cdot m\boldsymbol{\mathcal{V}}) \ln \left(1 + e^{-\beta(\epsilon_{n,\mathbf{k}} - \mathbf{k} \cdot \mathbf{v} - 2\mathbf{m}_n^{\text{orb}}(\mathbf{k}) \cdot m\boldsymbol{\mathcal{V}})} \right). \quad (\text{C8})$$

The converse vortical effect refers to the response of orbital magnetization to velocity. In order to calculate the density of orbital magnetization, we differentiate the free energy density with respect to $2m\boldsymbol{\mathcal{V}}$ while keeping the temperature $T = \beta^{-1}$ fixed. This calculation leads to:

$$\begin{aligned} \mathbf{M}^{\text{orb}}(\mathbf{v}) &= -\frac{\delta F}{\delta(2m\boldsymbol{\mathcal{V}})}|_{\mathbf{v}=0} \\ &= \sum_n \int_{\mathbf{k}} \mathbf{m}_n^{\text{orb}}(\mathbf{k}) f(\epsilon_{n,\mathbf{k}}, \mathbf{v}) \\ &\quad + \frac{1}{\beta} \int_{\mathbf{k}} \boldsymbol{\Omega}_n(\mathbf{k}) \ln \left(1 + e^{-\beta(\epsilon_{n,\mathbf{k}} - \mathbf{k} \cdot \mathbf{v})} \right) \\ &\equiv \chi^{\text{orb}} \cdot \mathbf{v} + O(\mathbf{v}^2) \end{aligned} \quad (\text{C9})$$

where Fermi distribution function⁴⁴ $f(\epsilon_{n,\mathbf{k}}, \mathbf{v}) \equiv (e^{\beta(\epsilon_{n,\mathbf{k}} - \mathbf{k} \cdot \mathbf{v})} + 1)^{-1}$, and the tensor χ^{orb} representing the orbital magnetic susceptibility is denoted as:

$$\begin{aligned} \chi_{ij}^{\text{orb}} &= -\sum_n \int_{\mathbf{k}} m_{n,i}^{\text{orb}}(\mathbf{k}) f'(\epsilon_{n,\mathbf{k}}) k_j \\ &\quad + \sum_n \int_{\mathbf{k}} f(\epsilon_{n,\mathbf{k}}) \Omega_{n,i}(\mathbf{k}) k_j \equiv \chi_{ij}^{\text{Fs}} + \chi_{ij}^{\text{occ}} \end{aligned} \quad (\text{C10})$$

At $T = 0$, equation (C10) coincides with Eq. (13) in the main text. The Eq. (C10) reveals that the magnetic susceptibility is determined by the orbital magnetic moment of electrons on the Fermi surface (indicated as χ_{ij}^{Fs}) as well as the Berry curvature of the occupied bands (indicated as χ_{ij}^{occ}).

Appendix D: Kubo formula for orbital magnetic susceptibility

In this section, we present a derivation of the orbital magnetic susceptibility for a clean (disordered) electron fluid in both the static and uniform limit. The calculation is similar to the one that yields the vortical effect⁴⁵, which we refer the reader to for a more detailed description.

1. Orbital magnetic susceptibility as a functional of Green's function and current operator

In the continuum, the perturbation induced by the velocity field can be written as: $H_1 \equiv -i\mathbf{v}(\mathbf{r}, t) \cdot \nabla_{\mathbf{r}}$. In the Bloch basis, the perturbation matrix is composed of $\langle u_{m,\mathbf{k}} | \mathbf{k} | u_{n,\mathbf{k}+\mathbf{q}} \rangle \cdot \mathbf{v}(\mathbf{q}, t)$ and $\langle u_{m,\mathbf{k}} | (-i\nabla_{\boldsymbol{\rho}}) | u_{n,\mathbf{k}+\mathbf{q}} \rangle \cdot \mathbf{v}(\mathbf{q}, t)$. The first term arises from the plane wave component of the Bloch function $\psi_{\mathbf{k}}^n(\mathbf{r})$, while the second term is a result of the periodic part of the Bloch function. The details are as follows:

The Bloch wavefunction for the n -th band is generically of the form $\psi_{\mathbf{k}}^n(\mathbf{r}) \equiv \psi_{\mathbf{k}}^n(\mathbf{R} + \boldsymbol{\rho}) = N^{-1/2} e^{i\mathbf{k} \cdot (\mathbf{R} + \boldsymbol{\rho})} u_{n,\mathbf{k}}(\boldsymbol{\rho})$, where N is the number of unit cells, \mathbf{R} is a discrete index that labels them, $\boldsymbol{\rho}$ denotes position within a unit cell, and $u_{n,\mathbf{k}}(\boldsymbol{\rho})$ is periodic in $\boldsymbol{\rho}$ with the same periodicity as the underlying Hamiltonian. In this basis,

$$\langle \psi_{\mathbf{k}}^m | -i\mathbf{v}(\mathbf{r}, t) \cdot \nabla_{\mathbf{r}} | \psi_{\mathbf{k}+\mathbf{q}}^n \rangle = -i \int_{\mathbf{r}} \psi_{\mathbf{k}}^{m*}(\mathbf{r}) \mathbf{v}(\mathbf{r}, t) \cdot \nabla_{\mathbf{r}} \psi_{\mathbf{k}+\mathbf{q}}^n(\mathbf{r}) \quad (\text{D1})$$

Assuming $\mathbf{v}(\mathbf{r}, t) = e^{-i\mathbf{q}\cdot\mathbf{r}}\mathbf{v}(\mathbf{q}, t)$ and approximating $\mathbf{r} \sim \mathbf{R}$ and $\nabla_{\mathbf{r}} = \nabla_{\boldsymbol{\rho}}$, the matrix element becomes

$$\begin{aligned} \langle \psi_{\mathbf{k}}^m | -i\mathbf{v}(\mathbf{r}, t) \cdot \nabla_{\mathbf{r}} | \psi_{\mathbf{k}+\mathbf{q}'}^n \rangle &= -\frac{1}{N} \sum_{\mathbf{R}} e^{i(\mathbf{q}'-\mathbf{q})\cdot\mathbf{R}} \int_{\boldsymbol{\rho}, \boldsymbol{\rho}'} e^{-i\mathbf{k}\cdot\boldsymbol{\rho}+i(\mathbf{k}+\mathbf{q}'-\mathbf{q})\cdot\boldsymbol{\rho}'} [u_{m,\mathbf{k}}^*(\boldsymbol{\rho}) i\nabla_{\boldsymbol{\rho}} \delta(\boldsymbol{\rho}-\boldsymbol{\rho}') u_{n,\mathbf{k}+\mathbf{q}'}(\boldsymbol{\rho}')] \cdot \mathbf{v}(\mathbf{q}, t) \\ &= \frac{(2\pi)^3}{N} \sum_{\mathbf{K}} \delta(\mathbf{q}' - \mathbf{q} - \mathbf{K}) \left[\int_{\boldsymbol{\rho}} e^{i(\mathbf{q}'-\mathbf{q})\cdot\boldsymbol{\rho}} u_{m,\mathbf{k}}^*(\boldsymbol{\rho}) (\mathbf{k} - i\nabla_{\boldsymbol{\rho}}) u_{n,\mathbf{k}+\mathbf{q}'}(\boldsymbol{\rho}) \right] \cdot \mathbf{v}(\mathbf{q}, t) \\ &= \frac{(2\pi)^3}{N} \sum_{\mathbf{K}} \delta(\mathbf{q}' - \mathbf{q} - \mathbf{K}) \left[\int_{\boldsymbol{\rho}} e^{i\mathbf{K}\cdot\boldsymbol{\rho}} u_{m,\mathbf{k}}^*(\boldsymbol{\rho}) (\mathbf{k} - i\nabla_{\boldsymbol{\rho}}) u_{n,\mathbf{k}+\mathbf{q}+\mathbf{K}}(\boldsymbol{\rho}) \right] \cdot \mathbf{v}(\mathbf{q}, t) \end{aligned} \quad (\text{D2})$$

where \mathbf{K} are reciprocal lattice vectors. Since $u_{n,\mathbf{k}+\mathbf{q}+\mathbf{K}}(\boldsymbol{\rho}) = e^{-i\mathbf{K}\cdot\boldsymbol{\rho}} u_{n,\mathbf{k}+\mathbf{q}}(\boldsymbol{\rho})$, the equation above can be expressed as follows:

$$\langle \psi_{\mathbf{k}}^m | -i\mathbf{v}(\mathbf{r}, t) \cdot \nabla_{\mathbf{r}} | \psi_{\mathbf{k}+\mathbf{q}'}^n \rangle = (2\pi)^3 \delta(\mathbf{q}' - \mathbf{q}) \left[\int_{\boldsymbol{\rho}} u_{m,\mathbf{k}}^*(\boldsymbol{\rho}) (\mathbf{k} - i\nabla_{\boldsymbol{\rho}}) u_{n,\mathbf{k}+\mathbf{q}}(\boldsymbol{\rho}) \right] \cdot \mathbf{v}(\mathbf{q}, t) \quad (\text{D3})$$

Each term in the sum over \mathbf{K} gives the same contribution and cancels the factor of N . Thus, we can safely assume \mathbf{q} and \mathbf{q}' to be within the first Brillouin zone and write

$$\langle \psi_{\mathbf{k}}^m | -i\mathbf{v}(\mathbf{r}, t) \cdot \nabla_{\mathbf{r}} | \psi_{\mathbf{k}+\mathbf{q}}^n \rangle = (2\pi)^3 \langle u_{m,\mathbf{k}} | (\mathbf{k} - i\nabla_{\boldsymbol{\rho}}) | u_{n,\mathbf{k}+\mathbf{q}} \rangle \cdot \mathbf{v}(\mathbf{q}, t) \equiv (2\pi)^3 \langle u_{m,\mathbf{k}} | \hat{\mathbf{Q}} | u_{n,\mathbf{k}+\mathbf{q}} \rangle \cdot \mathbf{v}(\mathbf{q}, t) \quad (\text{D4})$$

These are the matrix elements of the perturbation in the Bloch basis, and they enter into Kubo's formula, giving the orbital magnetization response to an external velocity field.

The orbital magnetization response to an external velocity field is captured by the response function, which can be expressed as a function of the Green's function and current operator :

$$\chi_{ij}^{\text{orb}}(\mathbf{q}, iq_n) = -\frac{1}{2} \epsilon_{i\mu\nu} i \partial_{q_\mu} T \sum_{i\nu_n} \int_{\mathbf{k}} \text{tr} [J_\nu(\mathbf{k} + \mathbf{q}) G_0(\mathbf{k}, i\nu_n) \hat{Q}_j G_0(\mathbf{k} + \mathbf{q}, i\nu_n + iq_n)], \quad (\text{D5})$$

Here, $G_0(\mathbf{k}, i\nu_n)$ represents the standard unperturbed Matsubara Green's function, defined as $[i\nu_n - H_0(\mathbf{k}) + i\text{sgn}(\nu_n)/2\tau]^{-1}$, where $H_0(\mathbf{k})$ denotes the unperturbed Hamiltonian. The ν -th component of the current operator is denoted as J_ν and is given by $\frac{\partial H_0}{\partial k_\nu}$. Furthermore, we introduce $\hat{\mathbf{Q}} \equiv \hat{\mathbf{k}} - i\nabla_{\boldsymbol{\rho}}$, where $i\nabla_{\boldsymbol{\rho}}$ represents the modification arising from the lattice background⁴⁵. In the continuum limit, $\hat{\mathbf{Q}}$ converges to $\hat{\mathbf{k}}$.

2. Magnetic susceptibility under different limits

After establishing the connection between the magnetic susceptibility and the Green's function, we will provide detailed steps for deriving the final expression of the magnetic susceptibility and analyze its behavior under different limits. Substituting the expression of $G_0 = [i\nu_n - H_0(\mathbf{k}) + i\text{sgn}(\nu_n)/2\tau]^{-1}$ into the Eq. (D5) for the magnetic susceptibility and defining $\mathbf{Q}^{mn} \equiv \langle u_{m,\mathbf{k}} | \hat{\mathbf{Q}} | u_{n,\mathbf{k}+\mathbf{q}} \rangle$, we obtain:

$$\chi_{ij}^{\text{orb}}(\mathbf{q}, iq_n) = -\frac{1}{2} \epsilon_{i\mu\nu} i \partial_{q_\mu} T \sum_{i\nu_n} \int_{\mathbf{k}} \sum_{n,m} \frac{\langle u_{n,\mathbf{k}+\mathbf{q}} | J_\nu(\mathbf{k} + \mathbf{q}) | u_{m,\mathbf{k}} \rangle}{(i\nu_n - \epsilon_{m,\mathbf{k}} + i\frac{\text{sgn}(\nu_n)}{2\tau})} \frac{Q_j^{mn}}{(i\nu_n + iq_n + \epsilon_{n,\mathbf{k}+\mathbf{q}} + i\frac{\text{sgn}(\nu_n+q_n)}{2\tau})}, \quad (\text{D6})$$

which can be simplified as :

$$\begin{aligned} \chi_{ij}^{\text{orb}}(\mathbf{q}, \omega) &= -\frac{i}{2} \epsilon_{i\mu\nu} \int_{\mathbf{k}} \sum_{n,m} [\partial_{q_\mu} S_{m,n}(\mathbf{k}, \mathbf{q}, iq_n)] \langle u_{n,\mathbf{k}+\mathbf{q}} | J_\nu(\mathbf{k} + \mathbf{q}) | u_{m,\mathbf{k}} \rangle Q_j^{mn} \\ &\quad - \frac{i}{2} \epsilon_{i\mu\nu} \int_{\mathbf{k}} \sum_{n,m} S_{m,n}(\mathbf{k}, \mathbf{q}, iq_n) [\partial_{q_\mu} \langle u_{n,\mathbf{k}+\mathbf{q}} | J_\nu(\mathbf{k} + \mathbf{q}) | u_{m,\mathbf{k}} \rangle Q_j^{mn}], \end{aligned} \quad (\text{D7})$$

where $|u_{n,\mathbf{k}}\rangle$ and $\epsilon_{n,\mathbf{k}}$ are the Bloch eigenfunction and eigenenergy of the band n , respectively, and the factor

$$S_{m,n}(\mathbf{k}, \mathbf{q}, iq_n) = T \sum_{i\nu_n} \frac{1}{\left(i\nu_n - \epsilon_{m,\mathbf{k}} + i\frac{\text{sgn}(\nu_n)}{2\tau}\right)} \frac{1}{\left(i\nu_n + iq_n - \epsilon_{n,\mathbf{k}+\mathbf{q}} + i\frac{\text{sgn}(\nu_n+q_n)}{2\tau}\right)}, \quad (\text{D8})$$

Performing the Matsubara summation and the analytical continuum $iq_n \rightarrow \omega + i0^+$, we get

$$S_{m,n}(\mathbf{k}, \mathbf{q}, \omega) = - \int dz \text{Im} \left[\frac{2}{z + \frac{i}{2\tau}} \right] \frac{f(\epsilon_{m,\mathbf{k}} + z) - f(\epsilon_{n,\mathbf{k}+\mathbf{q}} - z)}{z + \epsilon_{m,\mathbf{k}} - \epsilon_{n,\mathbf{k}+\mathbf{q}} + \omega + \frac{i}{2\tau}}, \quad (\text{D9})$$

At the limit $(\mathbf{q}, \omega) \rightarrow (\mathbf{0}, 0)$, we get:

$$\begin{aligned} \chi_{ij}^{\text{orb}}(\mathbf{0}, 0) &= -\frac{i}{2} \epsilon_{i\mu\nu} \int_{\mathbf{k}} \sum_{n,m} \left[\frac{dS_{m,n}(\mathbf{k}, \mathbf{0}, 0)}{d\epsilon_{n,\mathbf{k}}} \partial_\mu \epsilon_{n,\mathbf{k}} \right] \langle u_{n,\mathbf{k}} | \partial_\nu H_0(\mathbf{k}) | u_{m,\mathbf{k}} \rangle Q_j^{mn} \\ &\quad - \frac{i}{2} \epsilon_{i\mu\nu} \int_{\mathbf{k}} \sum_{n,m} S_{m,n}(\mathbf{k}, \mathbf{0}, 0) \left[\langle \partial_\mu u_{n,\mathbf{k}} | \partial_\nu H_0(\mathbf{k}) | u_{m,\mathbf{k}} \rangle Q_j^{mn} + \langle u_{n,\mathbf{k}} | \partial_\nu H_0(\mathbf{k}) | u_{m,\mathbf{k}} \rangle \langle u_{m,\mathbf{k}} | \hat{Q}_j | \partial_\mu u_{n,\mathbf{k}} \rangle \right]. \end{aligned} \quad (\text{D10})$$

Note that the expression of $S_{m,n}(\mathbf{k}, \mathbf{0}, 0)$ depends on the order of limits, which we will clarify shortly. At zero temperature and to leading order in τ^{-1} , the factor $S_{m,n}(\mathbf{k}, \mathbf{0}, 0) = \frac{\Theta(-\epsilon_{m,\mathbf{k}}) - \Theta(-\epsilon_{n,\mathbf{k}})}{\epsilon_{m,\mathbf{k}} - \epsilon_{n,\mathbf{k}}}$ for $m \neq n$, and $S_{n,n}(\mathbf{k}, \mathbf{0}, 0) = -\delta(\epsilon_{n,\mathbf{k}})$ or 0. Using the relations

$$\langle u_{n,\mathbf{k}} | \partial_\nu H_0(\mathbf{k}) | u_{m,\mathbf{k}} \rangle = -(\epsilon_{n,\mathbf{k}} - \epsilon_{m,\mathbf{k}}) \langle u_{n,\mathbf{k}} | \partial_\nu u_{m,\mathbf{k}} \rangle + \delta_{n,m} \partial_\nu \epsilon_{n,\mathbf{k}}, \quad (\text{D11})$$

and

$$\langle u_{n,\mathbf{k}} | \partial_\nu H_0(\mathbf{k}) | \partial_\theta u_{m,\mathbf{k}} \rangle = \epsilon_{n,\mathbf{k}} \langle \partial_\nu u_{n,\mathbf{k}} | \partial_\theta u_{m,\mathbf{k}} \rangle - \langle \partial_\nu u_{n,\mathbf{k}} | H_0(\mathbf{k}) | \partial_\theta u_{m,\mathbf{k}} \rangle + \partial_\nu \epsilon_{n,\mathbf{k}} \langle u_{n,\mathbf{k}} | \partial_\theta u_{m,\mathbf{k}} \rangle. \quad (\text{D12})$$

The first term on the right-hand side of Eq. (D10) can be expressed as follows:

$$-\frac{i}{2} \epsilon_{i\mu\nu} \int_{\mathbf{k}} \sum_{n \neq m} [\delta(\epsilon_{m,\mathbf{k}}) + S_{m,n}(\mathbf{k}, \mathbf{0}, 0)] \langle \partial_\mu u_{m,\mathbf{k}} | \partial_\nu \epsilon_{m,\mathbf{k}} | u_{n,\mathbf{k}} \rangle Q_j^{nm}, \quad (\text{D13})$$

and the second term on the right-hand side of Eq. (D10) can be expressed as follows:

$$\begin{aligned} &-\frac{i}{2} \epsilon_{i\mu\nu} \int_{\mathbf{k}} \sum_{n \neq m} S_{m,n}(\mathbf{k}, \mathbf{0}, 0) \left[\langle \partial_\mu u_{m,\mathbf{k}} | \partial_\nu H_0(\mathbf{k}) | u_{n,\mathbf{k}} \rangle Q_j^{nm} + \langle u_{m,\mathbf{k}} | \partial_\nu H_0(\mathbf{k}) | u_{n,\mathbf{k}} \rangle \langle u_{n,\mathbf{k}} | \hat{Q}_j | \partial_\mu u_{m,\mathbf{k}} \rangle \right] \\ &-\frac{i}{2} \epsilon_{i\mu\nu} \int_{\mathbf{k}} \sum_n S_{n,n}(\mathbf{k}, \mathbf{0}, 0) \left[\langle \partial_\mu u_{n,\mathbf{k}} | (\epsilon_{n,\mathbf{k}} - H_0(\mathbf{k})) | \partial_\nu u_{n,\mathbf{k}} \rangle Q_j^{nn} \right] \\ &-\frac{i}{2} \epsilon_{i\mu\nu} \int_{\mathbf{k}} \sum_n S_{n,n}(\mathbf{k}, \mathbf{0}, 0) \partial_\nu \epsilon_{n,\mathbf{k}} \left[\langle u_{n,\mathbf{k}} | \hat{Q}_j | \partial_\mu u_{n,\mathbf{k}} \rangle + \langle \partial_\mu u_{n,\mathbf{k}} | u_{n,\mathbf{k}} \rangle Q_j^{nn} \right], \end{aligned} \quad (\text{D14})$$

Combining Eq. (D13) and Eq. (D14), finally, we obtain the expression for the magnetic susceptibility as:

$$\begin{aligned}
\chi_{ij}^{\text{orb}}(\mathbf{0}, 0) = & - \int_{\mathbf{k}} \sum_{n \neq m} S_{m,n}(\mathbf{k}, \mathbf{0}, 0) \mathcal{M}_i^{mn}(\mathbf{k}) Q_j^{nm} \\
& + \frac{1}{2} \epsilon_{i\mu\nu} \int_{\mathbf{k}} \sum_{n \neq m} S_{m,n}(\mathbf{k}, \mathbf{0}, 0) (\epsilon_{m,\mathbf{k}} - \epsilon_{n,\mathbf{k}}) \langle u_{m,\mathbf{k}} | \partial_\nu u_{n,\mathbf{k}} \rangle \langle u_{n,\mathbf{k}} | \partial_{\rho_j} | \partial_\mu u_{m,\mathbf{k}} \rangle \\
& + \frac{i}{2} \epsilon_{i\mu\nu} \int_{\mathbf{k}} \sum_{n \neq m} [S_{m,n}(\mathbf{k}, \mathbf{0}, 0) (\epsilon_{m,\mathbf{k}} - \epsilon_{n,\mathbf{k}})] [A_\nu^{nm}(\mathbf{k}) A_\mu^{mn}(\mathbf{k})] k_j \\
& - \frac{i}{2} \epsilon_{i\mu\nu} \int_{\mathbf{k}} \sum_n S_{n,n}(\mathbf{k}, \mathbf{0}, 0) [\langle \partial_\mu u_{n,\mathbf{k}} | (\epsilon_{n,\mathbf{k}} - H_0(\mathbf{k})) | \partial_\nu u_{n,\mathbf{k}} \rangle Q_j^{nn}] \\
& - \frac{i}{2} \epsilon_{i\mu\nu} \int_{\mathbf{k}} \sum_{n \neq m} \delta(\epsilon_{m,\mathbf{k}}) \langle \partial_\mu u_{m,\mathbf{k}} | \partial_\nu \epsilon_{m,\mathbf{k}} | u_{n,\mathbf{k}} \rangle Q_j^{nm} \\
& - \frac{i}{2} \epsilon_{i\mu\nu} \int_{\mathbf{k}} \sum_n S_{n,n}(\mathbf{k}, \mathbf{0}, 0) \partial_\nu \epsilon_{n,\mathbf{k}} [\langle u_{n,\mathbf{k}} | \hat{Q}_j | \partial_\mu u_{n,\mathbf{k}} \rangle + \langle \partial_\mu u_{n,\mathbf{k}} | u_{n,\mathbf{k}} \rangle Q_j^{nn}]. \tag{D15}
\end{aligned}$$

where \mathcal{M}_i^{mn} represents the inter-band orbital magnetization matrix for the Bloch electrons⁷³, which takes the following form,

$$\mathcal{M}_i^{mn}(\mathbf{k}) = \frac{i}{2} \epsilon_{i\mu\nu} [\langle \partial_\mu u_{m,\mathbf{k}} | (\partial_\nu H_0(\mathbf{k}) + \partial_\nu \epsilon_{m,\mathbf{k}}) | u_{n,\mathbf{k}} \rangle]. \tag{D16}$$

In some limit conditions, such as the nearly-free electron and deep tight-binding limits⁴⁵, the term $\langle u_{n,\mathbf{k}} | \partial_{\rho_j} u_{m,\mathbf{k}} \rangle$ is negligible, and Eq. (D15) can be further simplified as:

$$\begin{aligned}
\chi_{ij}^{\text{orb}}(\mathbf{0}, 0) = & - \sum_n \frac{i}{2} \int_{\mathbf{k}} S_{n,n}(\mathbf{k}, \mathbf{0}, 0) [\langle \nabla_{\mathbf{k}} u_{n,\mathbf{k}} | \times (\epsilon_{n,\mathbf{k}} - H_0(\mathbf{k})) | \nabla_{\mathbf{k}} u_{n,\mathbf{k}} \rangle]_i k_j \\
& + \frac{i}{2} \epsilon_{i\mu\nu} \int_{\mathbf{k}} \sum_{n \neq m} [S_{m,n}(\mathbf{k}, \mathbf{0}, 0) (\epsilon_{m,\mathbf{k}} - \epsilon_{n,\mathbf{k}})] [A_\nu^{nm}(\mathbf{k}) A_\mu^{mn}(\mathbf{k}) k_j]. \tag{D17}
\end{aligned}$$

The first term accounts for the contribution of the intra-band orbital magnetic moment to the orbital magnetization, while the second term reflects the dependence of the orbital magnetization on the Berry connection of the occupied bands. In the subsequent analysis, we assume the term $\langle u_{n,\mathbf{k}} | \partial_{\rho_j} u_{n,\mathbf{k}} \rangle$ is negligible and thoroughly examine the magnetic susceptibility under different limits, with a specific emphasis on the zero-temperature.

a. Static limit ($\omega \rightarrow 0$ before $\mathbf{q} \rightarrow \mathbf{0}$)

In the static limit, the factor $S_{m,n}$ can be written as⁴⁵:

$$S_{n,n}(\mathbf{k}, \mathbf{q} \rightarrow \mathbf{0}, 0) = \begin{cases} -\delta(\epsilon_{n,\mathbf{k}}) & |\nabla_{\mathbf{k}} \epsilon_{n,\mathbf{k}} \cdot \mathbf{q}\tau| \gg 1, \\ \frac{1}{\pi} \text{Im} \left[\frac{1}{\epsilon_{n,\mathbf{k}} + \frac{i}{2\tau}} \right] & |\nabla_{\mathbf{k}} \epsilon_{n,\mathbf{k}} \cdot \mathbf{q}\tau| \ll 1, \end{cases} \tag{D18}$$

$$S_{m,n}(\mathbf{k}, \mathbf{q} \rightarrow \mathbf{0}, 0) \approx \frac{\Theta(-\epsilon_{m,\mathbf{k}}) - \Theta(-\epsilon_{n,\mathbf{k}})}{\epsilon_{m,\mathbf{k}} - \epsilon_{n,\mathbf{k}}} \text{ for } m \neq n. \tag{D19}$$

where τ^{-1} quantifies the strength of disorder. By substituting this expression for factor $S_{m,n}$ into the Eq. (D15), and considering the leading order of τ^{-1} , we obtain

$$\begin{aligned}
\chi_{ij}^{\text{orb}}(\mathbf{k}, \mathbf{q} \rightarrow \mathbf{0}, 0) = & \sum_n \int_{\mathbf{k}} \delta(\epsilon_{n,\mathbf{k}}) m_i^{\text{orb}} k_j + \sum_n \int_{\mathbf{k}} \Theta(-\epsilon_{n,\mathbf{k}}) \Omega_n^i k_j \\
& \text{for } |\nabla_{\mathbf{k}} \epsilon_{n,\mathbf{k}} \cdot \mathbf{q}\tau| \gg 1, \tag{D20}
\end{aligned}$$

$$\chi_{ij}^{\text{orb}}(\mathbf{k}, \mathbf{q} \rightarrow \mathbf{0}, 0) = \sum_n \int_{\mathbf{k}} \delta(\epsilon_{n,\mathbf{k}}) m_i^{\text{orb}} k_j + \sum_n \int_{\mathbf{k}} \Theta(-\epsilon_{n,\mathbf{k}}) \Omega_n^i k_j \quad (\text{D21})$$

for $|\nabla_{\mathbf{k}} \epsilon_{n,\mathbf{k}} \cdot \mathbf{q}\tau| \ll 1$.

where $m_i^{\text{orb}} \equiv \frac{i}{2} [\langle \nabla_{\mathbf{k}} u_{n,\mathbf{k}} | \times (\epsilon_{n,\mathbf{k}} - H_0(\mathbf{k})) | \nabla_{\mathbf{k}} u_{n,\mathbf{k}} \rangle]_i$ denotes the i th component of the orbital moment, and Ω_n^α is the α th component of the Berry curvature $\mathbf{\Omega}_n \equiv \nabla_{\mathbf{k}} \times \mathbf{K}_n$ of n th band.

b. Uniform limit ($\mathbf{q} \rightarrow \mathbf{0}$ before $\omega \rightarrow 0$)

In the uniform limit, the factor $S_{m,n}$ can be written as:

$$S_{n,n}(\mathbf{k}, \mathbf{0}, \omega \rightarrow 0) = \begin{cases} 0 & |\omega\tau| \gg 1, \\ \frac{1}{\pi} \text{Im} \left[\frac{1}{\epsilon_{n,\mathbf{k}} + \frac{i}{2\tau}} \right] & |\omega\tau| \ll 1, \end{cases} \quad (\text{D22})$$

$$S_{m,n}(\mathbf{k}, \mathbf{0}, \omega \rightarrow 0) \approx \frac{\Theta(-\epsilon_{m,\mathbf{k}}) - \Theta(-\epsilon_{n,\mathbf{k}})}{\epsilon_{m,\mathbf{k}} - \epsilon_{n,\mathbf{k}}} \text{ for } m \neq n. \quad (\text{D23})$$

the factor $S_{m,n}$ is the same as in the static limit for the disorder case, however, the intra-band term $S_{n,n} = 0$ in the clean case. Finally, we obtain the susceptibility in uniform limit for clean and disorder case which is given by:

$$\chi_{ij}^{\text{orb}}(\mathbf{k}, \mathbf{0}, \omega \rightarrow 0) = \sum_n \int_{\mathbf{k}} \Theta(-\epsilon_{n,\mathbf{k}}) \Omega_{n,i} k_j, \quad \text{for } |\omega\tau| \gg 1, \quad (\text{D24})$$

$$\chi_{ij}^{\text{orb}}(\mathbf{k}, \mathbf{0}, \omega \rightarrow 0) = \sum_n \int_{\mathbf{k}} \delta(\epsilon_{n,\mathbf{k}}) m_i^{\text{orb}} k_j + \sum_n \int_{\mathbf{k}} \Theta(-\epsilon_{n,\mathbf{k}}) \Omega_{n,i} k_j \quad (\text{D25})$$

for $|\omega\tau| \ll 1$.